





NEUTRON DIFFRACTION RESEARCH IN NPI ASCR, V.V.I. IN ŘEŽ – HISTORY AND PRESENT STATUS

P. Mikula

*Nuclear Physics Institute AS CR, v. v. i. and Research Centre Řež, Ltd., 250 68 Řež
mikula@ujf.cas.cz*

Keywords:

neutron source, neutron diffraction, neutron radiography

Abstract

In 2007 we commemorate the 50th anniversary of starting the operation of the research reactor in Řež. Its commissioning in 1957 has opened a new area for scientists in the field of basic and applied neutron research. After construction of the first diffractometer SPN-100 it resulted in an enormous expansion of neutron scattering investigations. The present paper describes short description of the author of the history and the present status of activities in condensed matter investigations by neutron scattering.

Thermal neutron investigations at the Řež research reactor

Theoretical and experimental research in the field of neutron scattering started after the Second World War when first intensive neutron sources – nuclear research reactors were constructed. Soon, however, neutrons have appeared as excellent probes of all kinds of matter. At present, many variations of the scattering process are used which give the technique of neutron scattering enormously wide applicability in studies of structure and properties of the condensed matter. Therefore, at each research reactor or pulsed neutron source there are installed many dedicated experimental devices. This year it is just 50th anniversary of starting the operation of the research reactor in the former Czechoslovakia when the first chain reaction was realized in it on September 25, 1957. The commissioning of this reactor of the Russian type VVR-S and of the power of 2 MW belongs to the key milestones in the development of research activities in neutron physics (generally), reactor physics and production of radioisotopes in our country. Naturally, it has opened a new area for scientists in the field of basic and applied neutron research. Later on, after two reconstructions the present tank type and light water reactor LWR-15 operates at the mean power of 10 MW when using decreased ^{235}U - enrichment from 80 % to 36 %.

First neutron investigations were focused to pure nuclear and reactor physics. Even at present, three important research activities of the basic and interdisciplinary (or applied) research are carried out at the facilities installed at the reactor. Namely, they are: Thermal neutron depth profiling facility which is used as a nuclear analytical technique for surface studies. It utilizes the existence of isotopes of elements that produce prompt monoenergetic charged particles upon capture of thermal neutrons. From the energy loss spectra of emitted products the depth distributions of light elements can be reconstructed. Neutron activation analysis facility is dedicated to bNeutron Activation Analysis with short- and long-time irradiations

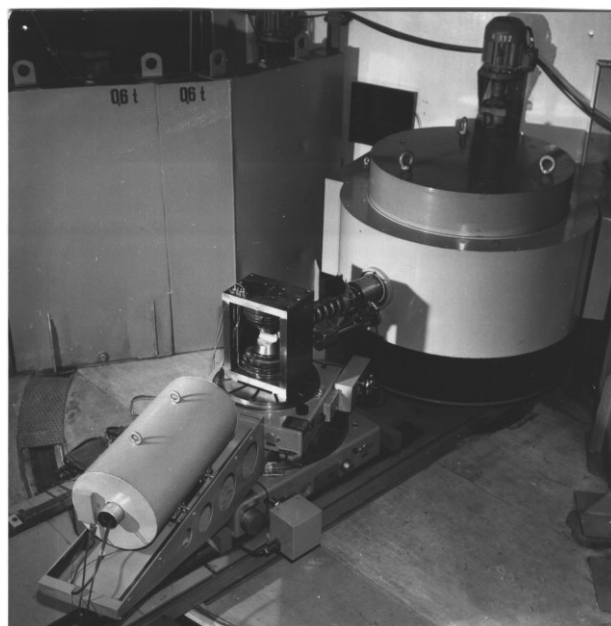


Figure 1. Diffractometer SPN-100 after its introduction into operation in 1965 for studies of magnetic properties of crystalline materials by polarized neutron diffraction.

performed in vertical channels of the reactor which are located at the outskirts of the reactor core. This technique provides a highly accurate and low-level characterization of various materials by determining up to 40 elements. Nuclear radiative capture facility is used for prompt gamma activation analysis and gamma-gamma coincidence measurements. The former investigations are focused mainly to analysis of ^{10}B in biological samples as an important part of the boron neutron capture therapy medical treatment and the latter ones to structure studies of nuclei. However, after construction of the first diffractometer SPN-100 in 1965, according to the trends in the world, an enormous expansion of investigations in the field of condensed matter physics and neutron optics by neutron scattering have been recorded. At present, there are installed 6 scattering devices of NPI ASCR at 5 horizontal beam channels of the reactor LWR-15. Besides the neutron optics the research program carried out at the diffractometers is mostly focused to material research as e.g. residual phase specific strain/stress studies, in-situ studies of martensitic transformation in shape memory alloys, studies of structure inhomogeneities by small-angle neutron scattering, texture measurements, etc. In 2005 the neutron interferometry investigations were stopped and instead of the interferometer facility a new multipurpose high and ultrahigh resolution diffractometer is constructed. Similarly, instead of the old facility for texture studies a new medium resolution powder diffractometer equipped with a multidetection system

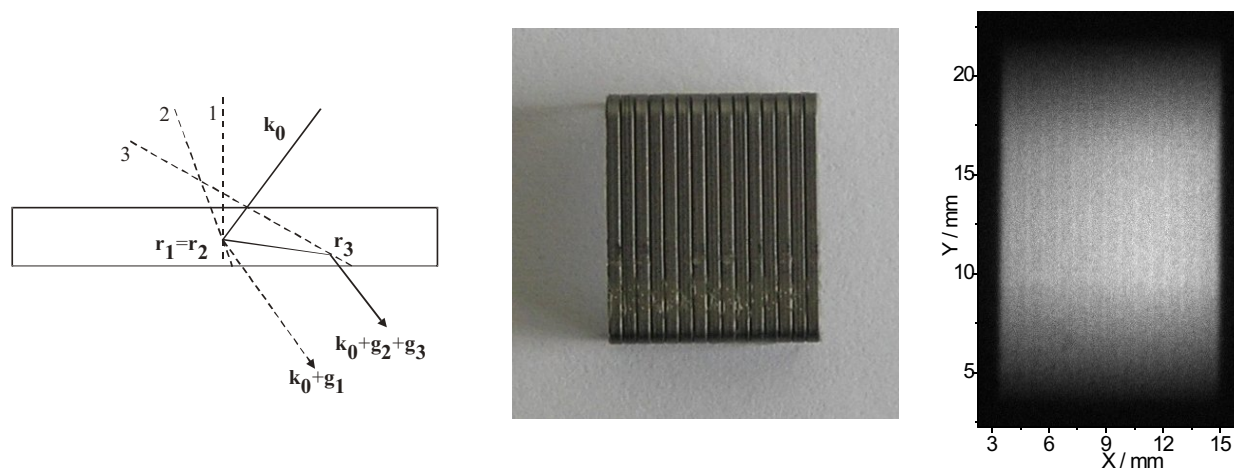


Figure 2. Schematic diagram of a two-step multiple Bragg reflection of neutron of the wave vector \mathbf{k}_0 simulating a weak or forbidden reflection (a) and an example of the radiography image (c) of the office staples 24/6 (b) taken by the image plate at the distance of 70 cm from the sample. The numbers 1, 2 and 3 correspond to the primary, secondary and tertiary reflection planes and \mathbf{g}_1 , \mathbf{g}_2 and \mathbf{g}_3 are the corresponding scattering vectors, respectively.

is installed. Both new diffractometers are expected to be fully operational until the end of 2007. Several experimental facilities are offered to external users in the frame of the FP6-NMI3 ACCESS Transnational Program. Fig. 2 shows the latest result of high resolution neutron radiography obtained on the newly constructed multipurpose diffractometer employing a special monochromator based on a strong dispersive double-reflection process [1-4]. The double reflection was excited in an elastically bent perfect Si-crystal. Such monochromator provides very high and resolution making and of the monochromatized beam very small without use of any collimators. In relation to the value of the bending radius, the obtained doubly reflected beam has a narrow band-width of 10^{-4} - 10^{-3} and θ -collimation of the order of minute of arc. This result shown in Fig. 2 is a demonstration of the new type of the so called phase contrast radiography based on the refraction contrast [5] which appears to be complementary to the absorption radiography.

References

1. Shih-Lin Chang, *Multiple Diffraction of X-rays in Crystals*, Springer Verlag, Berlin, 1984.
2. P. Mikula, M. Vrána, V. Wagner, *Physica B*, **350**, (2004), e667.
3. P. Mikula, M. Vrána, V. Wagner, *Zeitschrift für Kristallogr. Suppl.* **23**, (2006), 199.
4. P. Mikula, M. Vrána, In Proc. of the Int. Conf. ICEM-13, July 2-7, 2007, Alexandroupolis, ed. E. Gdoudos, in print.
5. N. Kardjilov, S.W. Lee, E. Lehmann, I.C. Lim, C.M. Sim, P. Vontobel, *Nucl. Instrum. Methods in Phys. Research A* **542**, (2005), 100.

Acknowledgements

Neutron research is supported by the projects AV0Z104 80505 and MSM2672244501.



PROGRAM

Pondělí, 18. 6.

11:30 - 13:00 Registrace

13:00 Zahájení

Strukturní databáze *I. Císařová, J. Brynda*

13.15

L1 p. 89

Radomír Kužel

Strukturní databáze anorganických struktur ICSD, CRYSTMET, PDF4, Pearson's Crystal Data a další volně dostupné strukturně zaměřené databáze na Internetu

14.00

L2 p. 97

Jindřich Hašek

Databáze organických struktur CSD a softwarové vybavení

14.45 Přestávka

15:10

L3 p. 101

Bohdan Schneider

Biostrukturní databáze PDB a NDB

15:40

L4

František Pavelčík p. 102

Automatické budování modelů proteinů a nukleových kyselin

16.10 Přestávka

Hlavní sál A

Studentská přehlídka I *V. Goliáš, J. Maixner*

16.30

S1 p. 127

Jan Rohlíček

Fox Grid - software pro urychlení řešení struktur z prášků metodou paralelního zpracování

16:50

S2 p. 127

Zdeněk Matěj

Rozšíření programu FOX pro analýzu mikrostruktury

17:10

S3 p. 127

Silvie Švarcová

Malířské pigmenty na bázi mědi, jejich chemismus a degradace

17:30

S4 p. 129

Ivana Jebavá

Porovnání výsledků mikrodifrakčních a makrodifrakčních experimentů na forenzních vzorcích

17.50

S5 p. 129

Richard Pažout

Structure determination of natural $\text{AgPbSbBi}_2\text{S}_6$ extracted from polished section

18.10

L15 p. 117

Martin Černík

Texture Analysis of rolled steel sheets by X-Ray and Electron Diffraction (EBSD)

Malý sál B

Kurs proteinové krystalografie

Měření na difraktometru, zpracování měření

B. Schneider

16:30

Jindřich Hašek

Úvodní poznámky. Organizace kurzu, instalace programů

16.40

Jiří Brynda

Principy měření proteinových struktur - difrakční experiment

17.40

Jan Dohnálek

Metody molekulárního nahrazení

Hlavní sál A

Panalytical User's meeting

M. Krupka

19.30

Martijn Fransen

New modules for Panalytical systems

Radomír Kužel

Different diffraction geometries - short introduction

Zdeněk Matěj p. 148

High-resolution setup

Experience from Almelo laboratories (position sensitive detectors, monochromators, thin film measurements)

P. Bezdička p. 150

Micro-diffraction with a mono-capillary: how to setup our experiment)

Radomír Kužel p. 151

Texture and stress measurement with the Eulerian cradle on MRD system, double-mirror setup

Malý sál B

Kurs proteinové krystalografie

Příprava počítačů pro kurs proteinové krystalografie

Instalace software na Linuxových počítačích



Úterý, 19. 6.

Hlavní sál A

7:00 Snídaně

Fázové transformace *J. Hybler*
8.30

L6 p. 118
Vladimír Šíma

Fázové transformace, fázové diagramy, diferenciální
 skenovací kalorimetrie

9.20
 L7 p. 118
Václav Janovec

Databáze materiálů s fázovými transformacemi

9.45 Přestávka

Hlavní sál A

**Difrakce za nestandardních podmínek, prášková
 difrakce, komerční prezentace**

J. Hybler, R. Kužel

10.15
 L8 p. 119
Hana Petříčková

Měření s vlhkostní komorou

10:40
 L9 p. 119
Roman Skála

Rozšíření programu FOX pro analýzu mikrostruktury

11:05
 L10 p. 120
Martin Kusý

Štruktúrna analýza s využitím programu MAUD

11.30
Burkhard Hoffmann
 EFG GmbH, Rigaku commercial presentation

12.00
Boris Mič
 Scientific Instruments, Brno, Komerční prezentace Bruker

Malý sál B

**Kurs proteinové krystalografie
 Krystalizace, řešení struktur**

F. Pavelčík

10:15
Ivana Kutá Smatanová p. 154

Přehled metod krystalizace proteinů

11.20
Jaromír Marek
 Metody rafinace strukturních parametrů (parametrizace,
 typy omezujících podmínek, příklady REFMAC,
 SHELXL, CNS, ARP/wARP, atd.)

12. 30 Oběd

Studentská přehlídka II *B. Schneider, J. Hašek*
13.30

S6 p. 130
Petr Kolenko

Glycosylation of IgG-Fc
13:50

S7 p. 131
Klára Šašková

The Influence of I47A Mutation on Reduced Susceptibility
 to the Protease Inhibitor Lopinavir

14:10
 S8 p. 131
Julie Wolfová

Strukturní studie flavoproteinů WrbA, zástupce nové
 proteinové rodiny

14:30
 S9 p. 132
Tatyana Prudnikova

Structural and functional studies of higher plants
 photosystem II

14.50
 S10 p. 133
Alena Stsiapanava

Crystallization study of three mutant haloalkane
 dehalogenases derived from dehalogenase DhaA of
Rhodococcus rhodochrous NCIMB 13064

15.10 Přestávka

Studentská přehlídka III *L. Čaplovič, M. Čerňanský*
15.30

S11 p. 134
Jan Drahoukoupil

Real structure depth profile of shot-peened surface of a cor-
 rosion-resistant steel

15:50
 S12 p. 135
Zdeněk Pala

X-ray diffraction study of distribution of macroscopic re-
 sidual stresses in surface layers of steels after grinding

16:10
 S13 p. 135
Andrey Chichev

New neutron powder diffractometer in NPI Řež

16:30
 S14 p. 136
Vadim Davydov

In situ neutron diffraction studies of the microstructure re-
 sponse of the plain ferritic steel on tensile straining

16.50 Přestávka

*M. Čerňanský, Z. Šourek***Hlavní sál A****17.10**

S15

p. 137

Viktoria Cherkaska

Severe plastic deformation of metals - microstructural studies

17:30

S16

p. 138

Romana Cízlová

X-ray Diffraction Analysis of Heat-Affected Particles of Tool Steel Ch3F12 Powder

17:50

S17

p. 139

Václav Valeš

Difuzní rtg rozptyl na defektech v monokrystalickém křemíku měřený za vyšších teplot

Tenké vrstvy*P. Mikulík, Z. Šourek***10.15**

L13

p. 67

David Rafaja

Microstructure analysis of nanocrystalline materials and nanocomposites using the combination of X-ray diffraction and transmission electron microscopy

11:00

L14

p. 122

Mojmír Meduňa

Interdiffusion in SiGe alloys studied by x-rays

11:25*Dušan Novotný, Pragolab*

Studium morfologie materiálů

Malý sál B**Malý sál B****Kurs proteinové krystalografie***J. Brynda***16:00***Jan Dohnálek*

Experimentální fázování (metody anomálního rozptylu a izomorfního nahrazení)

16.50 Přestávka**17.10***Petr Kolenko*

Stavění modelu do map elektronové hustoty (ARP/wARP, XFIT, atd.)

Kurs proteinové krystalografie**Cvičení na počítačích***J. Hašek***11:00***Jiří Brynda*

Zpracování měřených dat (MOSFLM+SCALA)

11.50*Jan Dohnálek*

Metody zpracování měřených dat a řešení struktury (fázového problému)

Hlavní sál A**18.30 Večeře**

20.30 Večerní Safari (podle zájmu)

Studentská přehlídka IV*Z. Šourek, P. Mikulík***11.50**

S18

p. 139

*Lea Nichtová*Strukturní studium vrstev TiO₂**12:10**

S19

p. 141

Lukáš Horák

Study of the structure of GaMnAs thin layers

12:30

S20

p. 142

Jan Krčmář

Rentgenová difrakce na polykrystalických multivrstvách v GID geometrii

12:50

S21

p. 142

Martin Mixa

Kinetic Monte Carlo simulation of quantum-dot nucleation in PbSe/PbEuTe multi

Středa, 20. 6.

7:00 Snídaně

Povrchy a tenké vrstvy*D. Rafaja***8.30**

L11

p. 103

Radomír Kužel

Krystalografie povrchů, stručný přehled metod pro studium struktury povrchů a tenkých vrstev

9.00

L12

p. 121

Ivan Oš ádal

Povrchové mikroskopie s atomovým rozlišením

9.50 Přestávka**13.15 Oběd****14.00 Volno, možnosti výletů****19.00 Shromáždění členů a přátel Krystalografické společnosti****19.30 Večeře**

**Čtvrtek, 21. 6.**

7:00 Snidaně

*J. Hašek***8.30**

L15

p. 108

Pavel Mikula

Neutron diffraction research in NPI ASCR, v.v.i. in Řež – history and present status

9.10

L16

p. 110

Radomír Kužel

Některé komerční programy pro zobrazování struktur a simulaci difraktogramů - Diamond, Crystallographica, Crystal Maker

9.50 Přestávka**Studentská přehlídka V***P. Bezdička, F. Pavelčík***10.10**

S22

p. 143

*Pavla Roupčová*Nucleation and growth of Fe nanoparticles embedded in ZrO₂ matrix at high temperature**10.30**

S23

p. 143

*Daniela Králová*Příprava a struktura nanotrubiček TiO₂**10.50**

S24

p. 143

*František Laufek*Synthesis and structure of CoGeTe and CoSn_{1.5}Te_{1.5}**11.10**

S25

p. 145

Jan Filip

Solid-state synthesis, structure and applications of potassium ferrate(VI)

11.30

S26

p. 146

Petr Kovář

Hydrotalcit interkalovaný benzoovou kyselinou, molekulární modelování a experiment

11.50

S27

p. 147

Marek Veteška

Hydrotalcit interkalovaný pyrentetrasulfonovou kyselinou, molekulární modelování a experiment

12.15 Oběd**Hlavní sál A***P. Bezdička, R. Kužel***13.30**

L17

p. 124

Lubomír Čaplovič

Analýza vplyvu parametrov naprašovania na kvalitatívne zloženie tvrdých povlakov

13:55

L18

p. 125

Jiří Marek

Rtg fázová analýza texturovaných 2-fázových vzorků

14:20

L19

p. 125

Jiří Had

Semikvantitativní metoda pro sledování tvorby transformačních produktů geopolymerů

14:45

L20

p. 126

Marian Čerňanský

Čtvrté momenty v profilové analýze

Malý sál B**Kurs proteinové krystalografie****Výsledky strukturní analýzy, databáze***M. Hušák***13:30***Bohdan Schneider*

p. 154

Deposice proteinových struktur do PDB a příslušný software

14.30*Jindřich Hašek*

Využití výsledků rentgenové strukturní analýzy (Parametrizace proteinu, parametrizace ligandů, solvatační obálka, strukturní databáze, hodnocení chyb, statistické zpracování)

15.00

Závěrečná diskuse ke kursu proteinové krystalografie

15.20

Vyhlášení výsledků studentské soutěže a závěr kolokvia

STRUKTURA 2007

Penzion za vodou, Dvůr Králové, 18. 6. - 21. 6, 2007

Lectures - Monday, June 18

L1 - L4

STRUCTURAL DATABASES

see pages 89 - 101

L5

TEXTURE ANALYSIS OF ROLLED STEEL SHEETS BY X-RAY AND ELECTRON DIFFRACTION (EBSD)

M. Černík, L. Hrabčáková, A. Leško

U. S. Steel Košice, s.r.o., Slovak Republic

The rolled IF and TRIP steel sheets were evaluated by X-ray and electron diffraction methods. Textures were measured by X-ray diffraction using texture goniometer with Mo X-ray tube, employing (110), (200) (112) and (103) crystallography planes. EBSD camera was used for texture measurements by electron diffraction. ODF – orientation distribution functions were calculated from texture-measured data by use of shf – spherical harmonic function, WIMV and ADC methods. Both, X-ray and EBSD data obtained very good agreements on texture characterizations of non-grain oriented (NGO) steels in relation to their magnetic properties. The EBSD methods allow obtaining more structural information: IPF maps, grain shape, size, crystal orientation of selected grains and others.

The partially annealed IF steel sheet sample EBSD analysis shows directly the texture of individual grains, X-ray diffraction method gives the material complex texture. EBSD method allows categorizing grains according to proper criteria. The criteria "Grain average disorientation" was used for grains categorizing into two groups; re-crystallized and deformed grains.

The rolled IF steel sample texture was formed by alpha and gamma fibers. The final texture was the superposition

of the deformation and recrystallization texture. The deformation texture was formed by uncompleted alpha fiber with (001) 011, (113) 011, (223) 011 texture elements. The recrystallization texture was formed by gamma fiber with (111) 011 to (111) 112 texture components.

The EBSD method allows analyzing samples with complex phase composition. Comparing the X-ray diffraction method, which is limited by material texture, the retained austenite content in rolled steel sheets can be directly and exactly determined by EBSD method. At the same time the texture is obtained for particular phases too, in this case the texture of ferrite and residual austenite. The EBSD method provides data about grain size and shape, boundaries characteristics for all present phases.

The rolled TRIP steel sample ferritic phase was formed by strong gamma fiber (111) 011 to (111) 112 and by small amount of (100) 011 and (110) 001 texture components. The retained austenite content was estimated for 5,2%. The residual austenite texture was formed by Goss - (110) 001, Brass - (110) 112 texture components and a small amount of Copper - (112) 111 component.



Lectures - Tuesday, June 19

L6

PHASE TRANSFORMATIONS, PHASE DIAGRAMS, DIFFERENTIAL SCANNING CALORIMETRY

Vladimír Šíma

Dept. of Physics of Materials, Charles University, Ke Karlovu 5, 121 16 Prague 2, Czech Republic
sima@met.mff.cuni.cz

Thermodynamical basis of phase transformations. Anomalies of thermophysical quantities. Classification of phase transformations. Equilibrium in heterogeneous systems. Gibbs phase rule. Common tangent construction. Lever rule. Tangential plane construction. Binary and ternary phase diagrams. Basic types of binary phase diagrams.

Thermal analysis – differential thermal analysis (DTA), differential scanning calorimetry (DSC).

Work is supported by a grant from Czech Grant Agency (GAČR 106/06/0019).

L7

DATABASES OF CRYSTALS WITH STRUCTURAL PHASE TRANSITIONS

Václav Janovec¹, Pawel E. Tomaszewski², Milan Čmelík¹, Lubor Machonský¹, Zdeněk Kluiber³

¹Technical University of Liberec, Hálkova 6, 461 17 Liberec

²Institute of Low Temperature and Structural Research, PAN, 50-950 Wrocław, Poland

³University of Hradec Králové, Faculty of Education, Rokitanského 62, 500 03 Hradec Králové
janovec@fzu.cz

Crystals with structural phase transitions (SPT's) exhibit unusual physical properties that are utilized in many technical applications (e.g. anisotropic ceramics, memories, sensors, transducers) and in other fields (e.g. earth sciences). Though basic structural data on SPT's can be found in existing structural databases (ICSD, CSD) special features and advanced theoretical background of SPT's call for a specialized database.

The most comprehensive listing of non-metallic crystals with SPT's is available in *Tomaszewski's database of structural phase transitions* [1,2]. This is a printed table in which each row (record) is related to one chemical formula of a crystal and columns (fields) give transition temperatures as well as the main available structural data of corresponding phases in between two neighbouring transitions. In updated version [2] about 4 300 crystals are recorded with more than 6 300 phase transitions and about 10 000 crystal phases observed at normal pressure. This presentation provides useful information about the appearance of SPT's in crystals but does not allow an efficient search.

This drawback can be partially removed if the records are arranged according to the symmetry changes at the SPT. Such tables have been created from the updated Tomaszewski's database [2]. In the first step only crystals which exhibit just a single SPT associated with a dissymmetrization (reduction of the space group symmetry) have been included. To increase the reliability of data only those SPT's have been taken into account for which structures of both phases are commensurate and are recorded in

the Inorganic Crystal Structure Database (ICSD). These restrictions drastically reduce the number of considered crystals (only 20% of crystal phases that appear in [2] have a structure solved and recorded in ICSD!). A table formed from these selected data constitutes a simple *Ferroic Phase Transition Database* which can provide answers to useful simple queries and from which some statistical conclusions can already be deduced [3].

Present effort concentrates on creation of *computerized relational databases of SPT's*. This approach makes use of recent advances in database techniques and can utilize the extensive theoretical knowledge on SPT's (see, e.g. [4]).

1. P. Tomaszewski, Structural phase transitions in crystals. I. Database. II. Statistical analysis. *Phase Transitions*, **38**, (1992), 127.
2. P. Tomaszewski, *Golden Book of Phase Transitions*, Phase transitions database PTDB, manuscript, 2002.
3. V. Janovec, P. Tomaszewski, L. Richterová, Z. Kluiber, Inverse database of phase transitions in crystals with a single phase transition. *Ferroelectrics*, **301**, (2004), 169.
4. *International Tables for Crystallography, vol. D*, edited by A. Authier (Dordrecht: Kluwer Academic Publishers), 2003, Part 3: Structural phase transitions.

Acknowledgement

This work has been partially supported by the grant 202/07/1289 of the Grant Agency of the Czech Republic..

L8

MEASUREMENT WITH VT-RH CHAMBER

H. Petříčková

Zentiva a.s., U kabelovny 130, 102 37 Praha 10 – Dolní Měcholupy, Česká Republika

Email: hana.petrickova@zentiva.cz

Powder diffraction patterns are the most fundamental, yet crucially important; application of XRPD is in identification or “fingerprinting” of crystalline phases in pharmaceutical industry [1]. Function of temperature and/or relative humidity can provide a direct means of characterizing the stability of a pharmaceutical material at defined temperature and relative humidity and the occurrence of hydration/dehydration processes [2]. Such a non-ambient diffraction experiments can be performed at any stage of the drug development process (API production, stability testing, formulation, storage...) to avoid further complications.

The object of presented study is to demonstrate the possible utilization of variable temperature and relative humidity XRPD to investigate hydration/dehydration process of the pharmaceutical material.

The behaviour of pharmaceutical hydrates has become the object of increasing interest over last two decades, primarily due to the potential impact of hydrates on development process and dosage form performance. Hydration of

the material also plays a role in bioavailability, influences dissolution, hardness of tablets or even processability. Interconversion between polymorphs and hydrates may occur as a function of temperature or of relative humidity or of both. During and after manufacturing even air moisture from the environment may change the hydration state of API in dosage form.

X-ray diffraction system with variable temperature and relative humidity was used. Instrumentation as well as obtained results will be discussed. The potential for interconversion during development was studied. Just different powder diffraction patterns can be used as an evidenced of change in the structure. Anyway, DSC and IR were used as complementary techniques to XRPD.

1. J. Bernstein: Polymorphism in molecular crystals, IUCr Monographs on Crystallography – 14, Oxford University Press, 2002.
2. H.G. Brittain: Polymorphism in Pharmaceutical Solids, Marcel Dekker, Inc. 1999.

L9

THERMAL EXPANSION OF TIS: ASSESSMENT OF MISCIBILITY WITH TROILITE (FES)

R. Skála¹, M. Drábek², T. Boffa-Ballaran³

¹Institute of Geology, ASCR, Rozvojová 269, 165 00 Praha 6

²Czech Geological Survey, Geologická 6, 152 00 Praha 5

³Bayerisches Geoinstitut, Universität Bayreuth, D-95440 Bayreuth, Germany
skala@gli.cas.cz

From meteorites - aubrites, in which otherwise lithophile elements behave as siderophiles due to strongly reducing conditions, titanium-rich iron monosulfides were reported in literature. For example, in the Bustee aubrite, the titanium-bearing troilite, associated with osbornite (TiN), heideite (FeTi₂S₄) and oldhamite (CaS), was found to contain 17.2 to 25.2 wt % Ti. In the Bishopville aubrite, the content of titanium in troilite is reported to be up to 5.7 wt % [1]. The crystal structures of troilite and TiS are not identical under ambient conditions. While troilite is hexagonal with space group is *P2c* and unit-cell dimensions $a \sim 5.97 \text{ \AA}$, $c \sim 11.76 \text{ \AA}$, $V \sim 362 \text{ \AA}^3$ [2], TiS adopts NiAs-type structure with space group *P6₃/mmc* and the unit cell parameters $a \sim 3.31 \text{ \AA}$, $c \sim 6.34 \text{ \AA}$, $V \sim 60.2 \text{ \AA}^3$ [3]. At elevated temperatures, however, the troilite structure transforms to NiAs-type structure as well [4]. Consequently, a relatively significant mutual solubility can be expected between FeS and TiS at temperatures above this phase transition. To evaluate the crystallographic limits for the TiS miscibility

in FeS we carried out a series of high-temperature unit-cell refinements for the former phase.

To collect the diffraction data we used an X'Pert PRO MPD Alpha-1 multi-purpose X-ray diffraction system equipped with an incident beam monochromator, Co tube, and X'Celerator detector. The material was a synthetic TiS prepared under controlled condition in an evacuated silica tube. The sample was heated in an HTK 1200 high-temperature chamber in an alumina sample holder. The holder spun. The NIST silicon internal standard was used for calibration. To prevent oxidation of the sample helium protecting atmosphere was utilized.

In Figure 1 we present results of high-temperature diffraction study of TiS for temperature range from 20 to 400 °C. Within the interval the parameter a and the cell volume increase monotonically whereas cell edge c has the opposite trend. This behavior is identical to that observed for (close-)stoichiometric FeS above the temperature of transition between 2H and 1C polytypes [4]. This observa-



tion substantiates a broad field of mutual solubility along FeS - TiS join at elevated temperatures. On the contrary, these results do not corroborate that phases described from aubrites possess the troilite type 2H structure; most probably the transformation which troilite undergoes at ca 100 °C causes the change in symmetry in Ti-containing minerals.

1. D.W. Mittlefehldt, T.J. McCoy, C.A. Goodrich, A. Kracher, in *Planetary Materials*, edited by J.J. Papike (Washington: Mineralogical Society of America), 1998, 195.
2. H.T. Evans *Science*, **167**, (1970), 621.
3. H. Hahn & B. Harde *Zeit. Anorg. Allgem. Chemie* **288**, (1956), 241.
4. E.N. Selivanov, A.D. Vershinin, R.I. Gulyaeva *Inorg. Materials*, **39**, (2003), 1097.

L10

THE STRUCTURE ANALYSIS USING PROGRAM MAUD

Martin Kusý

Ústav Materiálov, J. Bottu 23, 917 23 Trnava, Slovenská Republika,
e-mail: martin.kusy@stuba.sk

The structure determination from powder diffraction data using the Rietveld approach is in most cases tedious work. However, due to suitable software available long lasting calculations can be significantly shortened. Currently, variety of computer programs for this purpose is available either as freeware or on a commercial base. Nevertheless, the degree these programs help user in extracting the structural data may vary significantly. The shared computer programs based on the Rietveld method can be divided into two general categories from the point of processing basic Rietveld refinable parameters. First category contains number of examples of programs which provide user with a value of refined parameters, for example GSAS, DBWS or FullProf. On the other hand only few programs are available which directly list values of structural parameters determined after each refinement cycle. One of them is a Rietveld method based computer program MAUD.

Both approaches have advantages as well as drawbacks. The first group of programs necessarily needs to employ further processing of extracted parameters. On the other hand it means also opportunity for operator to treat and manipulate the raw parameters in order to extract specific structural information. Second group offers instant information about structural parameters which are considered as refined values. However, these are provided without possibility to interact with basic parameters known from the Rietveld approach. Certainly, number of supporters can be found for both categories of programs. This contribution is not aimed at finding the best group of programs. It would rather concentrate and highlight some of valuable functions and properties the computer program MAUD offers to an operator.

Maud – stands for Materials Analysis Using Diffraction is diffraction/reflectivity analysis program developed on

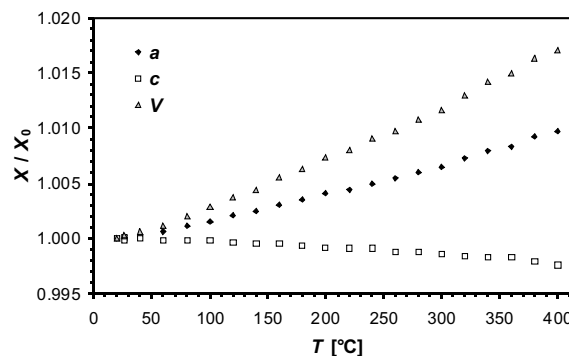


Figure 1. Relative changes of unit-cell dimensions in TiS at elevated temperature.

the basis of Rietveld method by Luca Lutterotti from University of Trento in Italy. This program is available since 1997. Maud is written in Java and can be executable in Windows, Mac OSX, Linux or Unix with pre-installed Java VM 1.4.

Author summarized the main features of the Maud program as follows:

- Easy to use, every action is controlled by a GUI
- Works with X-ray, synchrotron, Neutron, TOF
- Developed for Rietveld analysis, simultaneous multi spectra and different instruments/techniques supported
- Ab-initio structure solution integration, from peak finding, indexing to solving
- Different optimization algorithms available (LS, Evolutionary, Simulated Annealing, Metadynamics)
- Le Bail fitting
- Quantitative phase analysis
- Microstructure analysis (size-strain, anisotropy and distributions included)
- Texture and residual stress analysis using part or full spectra
- MEM algorithm for Electron Density Maps and fitting
- Thin film and multilayer aware; film thickness and absorption models
- Reflectivity fitting by different models, from Parratt (Matrix) to Discrete Born Approximation
- Several data files input formats
- Works and input images from 2D detectors (image plates, CCD)

- CIF compliance for input/output; import structures from databases

Our experience with the structure analysis of bulk steels or steel powders usually leads to application of quantitative phase analysis, microstructure analysis, texture analysis. In case of coated steel sheets, film thickness was determined successfully.

Due to simple user interface and available wizard the quantitative phase analysis can be performed using Maud in an intuitive way via releasing set of refinable parameters in five easy steps. Advanced users have opportunity to control each parameter separately.

For the purpose of microstructure analysis, Maud allows to use isotropic Delf model, anisotropic models with no rules and anisotropic model with Popa rules. Warren models for antiphase boundary and planar defects are also implemented in the code.

User can find also effective tools for compensation the texture of material. For this purpose, models such as March-Dollase, Harmonic functions, E-WIMV, WIMV are available. Experience shows that in most cases harmonic functions tends to be effective only when fiber symmetry as simplest one is engaged. The lower the symmetry the more of unstable parameters usually appears. E-WIMV and WIMV modules, allows the texture to be determined using Beartex from texture measurements and imported afterwards. Bearing in mind the drawback of harmonic func-

tions to import data from Beartex appears to be a safest way of texture compensation.

The Maud program provides user effective tool to characterize layers or multilayers deposited on single or multiphase substrate with possibility of thickness determination. For this purpose, the expected structure, phase constitution, ordering of layers and thickness is designed via available program interface. All mentioned layer properties can be during program execution handled as refinable parameters.

The Maud program is effective tool for structure analysis using diffraction. In general, it offers user friendly interface with the real-time pattern refinement monitor. Wider application of this program in scientific community is probably hindered with fact that there is no user guide available at the moment. Existing tutorials, Maud forum and Download section can be found at <http://www.ing.unitn.it/~maud/index.html>.

L. Lutterotti, S. Matthies and H. -R. Wenk, "MAUD (Material Analysis Using Diffraction): a user friendly Java program for Rietveld Texture Analysis and more", Proceeding of the Twelfth International Conference on Textures of Materials (ICOTOM-12), Vol. 1, 1599, (1999)

Acknowledgement

Financial support of the Slovak Grant Agency VEGA provided to project 1/4107/07 is acknowledged.

Lectures - Wednesday, June 20

L11

(see page 103 for more)

L12

SCANNING PROBE MICROSCOPY TECHNIQUES WITH ATOMIC RESOLUTION

Ivan Oš ádal

Department of Surface and Plasma Science, Faculty of Mathematics and Physics, Charles University in Prague, V Holešovičkách 2, 182 00 Praha 8, Czech Republic

Scanning tunneling microscopy (STM), atomic force microscopy (AFM) and related scanning probe microscopy (SPM) techniques developed during the last two decades are widely used for studying material surfaces. Information on surface structure with atomic resolution provided by imaging in real space considerably helped to elucidate a number of open questions and introduced new concepts into studying surface processes and crystal growth. STM technique (limited on conductive materials) can be modified for tunneling electron spectroscopy and used for investigation of local electron structure at surface. Dynamical measurements – imaging the surface at changing sample temperature or even during deposition of growing material – allow direct studying of phase transitions, behavior of individual atoms at surface diffusion, nucleation and growth. STM installed into ultrahigh vacuum chamber with various deposi-

tion and other techniques for surface analysis represents a powerful tool for complex experiments in surface science. AFM is the most used SPM technique especially due to variability of measuring modes, possibility of using various interactions for imaging sample surface and measurement at ambient conditions. Well defined atomically resolved measurements require ultrahigh vacuum conditions. AFM images obtained in this way can be interpreted with the help of theoretical models and chemical resolution is possible.

The contribution is focused on STM and AFM methods with respect of imaging surfaces with atomic resolution. It provides information on conditions and limitations of imaging, a comparison with other techniques and new prospects.



L13

MICROSTRUCTURE ANALYSIS OF NANOCRYSTALLINE MATERIALS AND NANOCOMPOSITES USING THE COMBINATION OF X-RAY DIFFRACTION AND TRANSMISSION ELECTRON MICROSCOPY

D. Rafaja¹, V. Klemm¹, C. Wüstefeld¹, M. Motylenko¹, M. Dopita^{1,2}

¹*Institute of Materials Science, TU Bergakademie Freiberg, Gustav-Zeuner-Str. 5, D-09599 Freiberg, Germany*

²*Department of Condensed Matter Physics, Charles University Prague, Ke Karlovu 5, CZ-121 16 Prague 2, Czech Republic*

Corresponding author: rafaja@ww.tu-freiberg.de

The capability of the combination of the X-ray diffraction and the transmission electron microscopy for the microstructure investigations on thin film and bulk nanocomposites are illustrated on three experimental examples: two Cr-Al-Si-N coatings with different chemical compositions and one BN bulk nanocomposite. Using a modified kinematical diffraction theory that describes and explains the phenomenon of the partial crystallographic

coherence of crystallites, we could show that the analysis of the X-ray diffraction line broadening is able to reveal nanocrystalline domains organised in semi-coherent clusters, to determine the size of the nanocrystalline domains and the clusters, and to quantify the mutual orientation of the partially coherent crystallites within these clusters. (see page 67 for more).

L14

INTERDIFFUSION IN SIGE ALLOYS STUDIED BY X-RAYS

M. Meduňa¹, J. Novák¹, G. Bauer², V. Holý³, C.V. Falub⁴, S. Tsujino⁴, D. Grützmacher⁴

¹*Institute of Condensed Matter Physics, Masaryk University, Kotlářská 2, 611 37 Brno, Czech Republic*

²*Institut für Halbleiterphysik, J Kepler Universität, Altenbergerstrasse 69, A-4040 Linz, Austria*

³*Faculty of Mathematics and Physics, Charles University, Ke Karlovu 5, 121 16 Prague, Czech Republic*

⁴*Laboratory for Micro- and Nanotechnology, Paul Scherrer Institut, CH-5232 Villigen PSI, Switzerland
mjme@physics.muni.cz*

A growing importance of SiGe-based electronic and of optoelectronic devices in recent past is evident due to a significant progress in Si/SiGe band gap and strain engineering [1]. Devices such as MOSFETs are one of these, which attract their attention very intensively due to their application in CMOS circuits. Quantum cascade lasers and light emitters gain their interest for its current threshold and low power consumption. The production of light emitters have been already mastered to a certain extent in III-V materials, but making of optoelectronic devices on the basis of IV-IV materials is more challenging because of their compatibility to a standard Si technology [2].

A typical obstacle that has to be overcome in design, processing and operation of all electronic devices is the thermal load during fabrication and during operation. Due to heat dissipation in the circuits and operation of devices at high temperatures, the diffusion processes of the materials has to be taken into account. Thus a detailed knowledge of the diffusion in SiGe alloys is highly desirable. Unfortunately the interdiffusion process in SiGe is unlinear and strongly depends on Ge concentration [3]. The parameters describing precisely the SiGe intermixing are still under investigation.

The interdiffusion coefficient of mixtures can be described by Arrhenius equation $D = D_0 \exp(E_A/kT)$ given by

activation energy E_A and diffusion pre-exponential factor D_0 . The non-linearity of the diffusion process in SiGe alloys consists in the strong dependence of E_A and D_0 on the Ge concentration X_{Ge} in $Si_{1-x}Ge_x$ [3,4]. Up to now only activation energies E_A and diffusion prefactors D_0 for X_{Ge} up to Ge contents of 50% were reported with comparatively large error bars [4]. Recently the authors Aubertine et al. have performed a systematic measurement of interdiffusion in SiGe multilayers with estimation of E_A and D_0 for $0 < X_{Ge} < 0.20$ with relatively small experimental error [5]. To our knowledge the parameters E_A and D_0 for $Si_{1-x}Ge_x$ in the range of X_{Ge} from 0.5 to 1 are not well reported.

The aim of our investigation was to extend the knowledge about SiGe interdiffusion process also for the range of Ge content from 25 % to 50 % and to determine new values of E_A and D_0 . We have annealed simple $Si_{1-x}Ge_x$ multilayers grown by molecular beam epitaxy on relaxed SiGe pseudosubstrate with graded Ge content from pure Si up to constant composition top layer. The multilayer itself consisted nominally from 30 periods of SiGe/Si bilayers sandwiched in between a 20 nm thick step graded layer system and covered by an additional SiGe cap layer due to strain symmetrization. More about the sample structure and

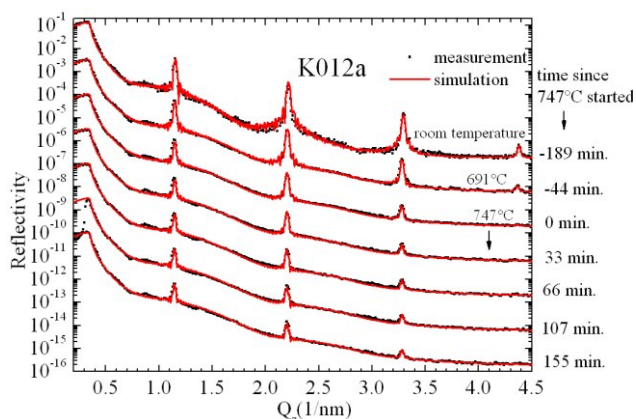


Figure 1. Evolution of x-ray reflectivity during annealing of $\text{Si}_{0.7}\text{Ge}_{0.3}/\text{Si}$ multilayer at $747\text{ }^\circ\text{C}$.

about the experiment can be found in our recent publication [6].

In order to study the diffusion properties of SiGe alloys in multilayer structures, we have used in-situ x-ray reflectivity and diffraction techniques performed at ESRF at beamline BM20. The critical temperature, where the interdiffusion started to be observable in our multilayers, was around $700\text{ }^\circ\text{C}$ and thus we have performed several isothermal annealing measurements above this temperature in order to obtain activation energy E_A and diffusion pre-exponential factor D_0 . Reciprocal space maps were recorded at several stages of annealing and for several temperatures mostly around $800\text{ }^\circ\text{C}$. The diffusion coefficients were obtained from the Ge content profile and from the profile of electron density, which were determined from

simulations of specular reflectivity and diffraction data, see Fig. 1.

The results were compared with data recently published by Aubertine *et al.* [5], who report diffusion coefficients showing linear decrease of activation energy and exponential decrease with Ge concentration. Our experiments show good agreement with extrapolation of these data [6] for Ge contents 50 % and 25 %. This statement suggests further generalization whether the dependency of E_A or D_0 is linear or exponential for the whole range of Ge content.

1. D. Paul, *Physics World*, 13, 27 (2000).
2. S. Tsujino, A. Borak, E. Müller, M. Scheinert, C.V. Falub, H. Sigg, D. Grützmacher, M. Giovannini, J. Faist, *Appl. Phys. Lett.*, **86**, (2006), 62113.
3. N. R. Zangenberg, J. Lundsgaard Hansen, J. Fage-Pedersen & A. Nylandsted Larsen, *Phys. Rev. Lett.*, **87**, (2001), 125901.
4. D.B. Aubertine, M.A. Mander, N. Ozguven, A.F. Marshall, P.C. McIntyre, J. O. Chu, P. M. Mooney, *J. Appl. Phys.*, **92**, (2002), 5027.
5. D.B. Aubertine & P.C. McIntyre, *J. Appl. Phys.*, **97**, (2005), 13531.
6. M. Meduňa, J. Novák, G. Bauer, V. Holý, C.V. Falub, S. Tsujino & D. Grützmacher, *Semicond. Sci. Technol.*, **22**, (2007), 447.

Acknowledgements

This work was supported by SANDiE (NMP4-CT-2004-500101), by the projects MSM0021622410 and MSM0021620834 of the Ministry of Education of Czech Republic and Grant Agency of Czech Republic (project no 202/05/P286).

Lectures - Thursday, June 21

L15

See page 108 for more

L16

See page 110 for more



L17

ANALÝZA VPLYVU PARAMETROV NAPRAŠOVANIA NA KVALITATÍVNE ZLOŽENIE TVRDÝCH POVLAKOV

L. Čaplovič¹, J. Sondor², J. Šimko³

¹Ústav materiálov, Materiálovotechnologická fakulta STU, Trnava, Slovenská republika

²LISS, a.s., Rožnov pod Radhoštěm, Česká republika

³PSA, a.s., Trnava, Slovenská republika
lubomir.caplovic@stuba.sk

V odbornej literatúre sme nenašli príspevky, ktoré by boli zamerané na sledovanie parametrov PVD naprašovania na tvorbu vrstvy. Väčšina autorov sa venuje kvalitatívnemu a kvantitatívnemu hodnoteniu PVD vrstiev vytvorených za predom definovaných podmienok [1-4]. V príspevku sa preto hodnotil vplyv predpätia a pracovného tlaku na kvalitatívne zmeny tvrdých vrstiev TiN/TiAlN vytvorených metódou PVD (konvenčný katódový oblúk) v zariadení PLATIT 1000. Rozsah použitých tlakov bol od 0,5 Pa do 5 Pa a hodnoty predpätia sa menili od 5 V do 500 V. Získané povlaky vytvorené na substráte spekaného karbidu (WC/Co) sa analyzovali pomocou rtg. difrakcie a to kvalitatívnou analýzou určujúcou fázové zloženie vytvorených vrstiev ako aj kvantitatívnym hodnotením difrakčných profilov, z ktorých sa analyzovala textúra povlakov a hodnota štruktúrnych napätí vo vrstvách.

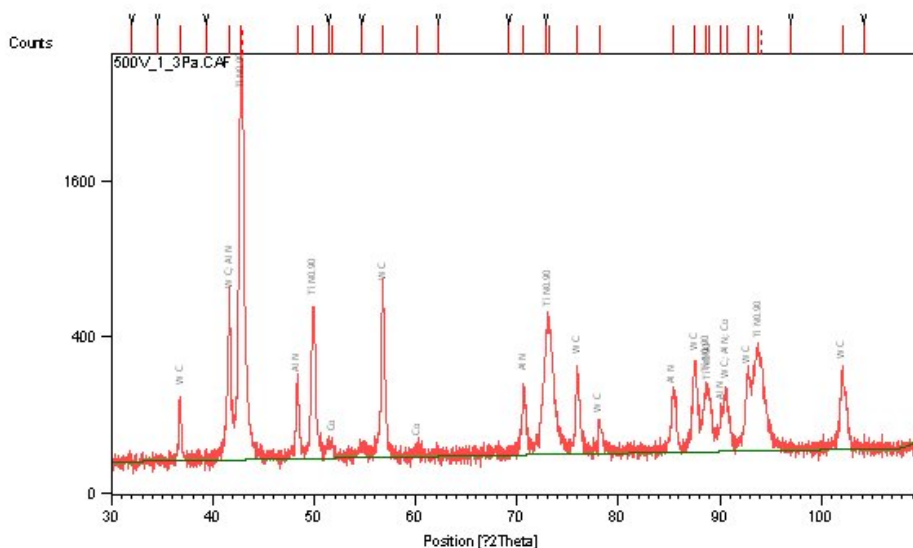
Ukázalo sa, že zmena parametrov naprašovania nemenila fázové zloženie vzniknutých vrstiev. Vo všetkých prípadoch sme detekovali prítomnosť nitridu titánu TiN_{0,9} a nitridu hliníka AlN, (AlTi)N. Substrát tvorila zmes karbidu volfrámu WC a Co. Difrakčný obraz pre parametre naprašovania (BIAS 500 V, p = 1,3 Pa) je na obr.1.

Zásadný vplyv zmeny predpätia sa prejavil v kvantitatívnom zložení vrstiev, stupni textúry a hodnote vnútorných štruktúrnych napätí vo vrstve. Kým nízke predpätia (5 a 25 V) vytvárali tenké vrstvy z relatívne nízkymi štruktúrными napätiami, pri dosiahnutí 75 V (100 V) bola vrstva optimálna z hľadiska hrúbky, ale mala

najvyššie hodnoty štruktúrnych napätí. Ďalšie zvyšovanie predpätia spôsobilo pokles hrúbky vrstvy v dôsledku vyššej kinetickej energie dopadajúcich iónov pôsobiacich odprašujúcim účinkom. Súčasne mierne klesala hodnota štruktúrnych napätí a textúry.

Zmena pracovného tlaku v naprašovacej komore sa výrazne neprejavila na nameraných difrakčných obrazoch vytvorených vrstiev.

1. J.L. Endrino, G.S. Fox-Rabinovich, C. Gey.: Hard AlTiN, AlCrN PVD coatings for machining of austenitic stainless steel, *Surface & Coatings Technology* **200** (2006) 6840–6845.
2. M. Arndt, T. Kacsich.: Performance of new AlTiN coatings in dry and high speed cutting, *Surface and Coatings Technology* **163–164** (2003) 674–680.
3. C. Ducros, C. Cayron, F. Sanchette.: Multilayered and nanolayered hard nitride thin films deposited by cathodic arc evaporation. Part I: Deposition, morphology and microstructure, *Surface & Coatings Technology* **201** (2006) 136–142.
4. C.V. Falub, A. Karimi, M. Ante, W. Kalss.: Interdependence between stress and texture in arc evaporated Ti–Al–N thin films, *Surface & Coatings Technology* **201** (2007) 5891–5898. Táto práca vznikla v rámci realizácie projektu EUREKA EURB-0005-06.



Obr. 1 Difrakčný obraz vytvorenej vrstvy na substráte spekaného karbidu

L18

KVANTITATIVNÍ RENTGENOVÁ DIFRAKČNÍ ANALÝZA DVOUFÁZOVÝCH TEXTUROVANÝCH VZORKŮ

J. Marek, Z. Pala, K. Kolařík

Department of Solid State Engineering, Faculty of Nuclear Sciences and Physical Engineering, Czech Technical University in Prague, Trojanova 13, 120 00 Prague 2

Základním problémem metodiky kvantitativní rentgenové difrakční fázové analýzy je texturovanost měřených vzorků, která mění intenzity difrakčních píků.

Pro fázovou analýzu byla použita bezstandardová metoda [1] pro dvoufázové netexturované vzorky. Texturovanost integrálních intenzit píků (hkl) obou fází je korigována pomocí faktorů $P(hkl)$ vypočtených Harrisovou metodou [2, 3]. Pro tuto metodiku jsou uvedeny matematické vztahy, výpočetní programy a jejich výsledky. Jsou uvedeny analýzy práškových vzorků

a vzorků s vysokým a nízkým stupněm texturovanosti a diskuse výsledků.

1. Fiala J. Absolutní stanovení objemového podílu alfa a gama fáze železa rentgenografickou metodou. 1967.
2. Harris, G. B.: *Phil.Mag.* **43** (1952) S.113-125.
3. Wasserman G., Grewen J.: *Texturen metallischer Werkstoffe*, Springer-Verlag 1962, S.94.

L19

SEMIQUANTITATIVE METHOD FOR THE MONITORING OF THE GEOPOLYMER TRANSFORMATION PRODUCTS

J. Had

Institute of Chemical Technology, Central laboratories, Prague

Synthetic geopolymers appear to be promising material applicable to a wide range of industrial branches, namely in building industry. Nevertheless products of geopolymer transformation can deteriorate properties of production. X-Ray phase analysis of geopolymers originating from thermal treated kaoline /metakaoline/ by alkaline treatment /NaOH and water glass/ has been carried out. Following products of the transformation have been identified: zeolite P, zeolite X, zeolite A, sodalite H and analcim T. A method for relative determination of the sum of the referred-to

phases has been worked out for the synthetic geopolymers, with respect to required quick determination and adequate accuracy. Data obtained in such way were collated with mechanical properties of the geopolymers arising from metakaolines at various temperatures of calcination and different ageing period, both at laboratory and 100°C temperature. Compression strength results correlated to the sums of the scaled intensities are presented proving applicability of the worked-out method.



L20

ČTVRTÉ MOMENTY V PROFILOVÉ ANALÝZE

M. Čerňanský

Fyzikální ústav AV ČR, v.v.i., Na Slovance 2, 182 21 Praha 8, Česká republika
cernan@fzu.cz

K popisu difrakčních profilů byly z matematické statistiky formálně převzaty některé veličiny charakterizující hustotu (rozložení) pravděpodobnosti $f(x)$ náhodné veličiny x . Motivem byla vnější podobnost tvarů hustot. Jednalo se zejména o momenty hustoty pravděpodobnosti, které jistým zhušňujícím způsobem charakterizují průběh, resp. tvar hustoty pravděpodobnosti:

$$M_0 = \int f(x) dx \quad \text{integrální intenzita,} \quad (1)$$

kteřou je rozumné normovat k 1, podobně jako je normovaná hustota pravděpodobnosti v matematické statistice. To umožňuje dále používat méně komplikované vztahy pro normované resp. redukované momenty (kolem počátku), které jsou definovány rovnicemi [1]

$$\begin{aligned} m_0 &= \int f(x) dx = 1 \\ m_1 &= \int x f(x) dx = T \text{ - těžiště} \\ m_2 &= \int x^2 f(x) dx \\ m_3 &= \int x^3 f(x) dx \\ m_4 &= \int x^4 f(x) dx \end{aligned} \quad (2)$$

Centrální momenty, vztažené k těžišti, pak vycházejí [1]

$$\begin{aligned} \mu_0 &= 1 \\ \mu_1 &= 0 \\ \mu_2 &= \int (x - m_1)^2 f(x) dx = m_2 - (m_1)^2 \quad W \text{ - variance} \\ \mu_3 &= m_3 - 3m_1 m_2 - (m_1)^3 \\ \mu_4 &= m_4 - 4m_1 m_3 - 6(m_1)^2 m_2 + 3(m_1)^4 \end{aligned}$$

Důležitou vlastností momentů je, že pokud funkce h je konvolucí funkcí f a g , pak pro těžiště a pro variance platí [2]

$$T_h = T_f + T_g \quad (4)$$

a

$$W_h = W_f + W_g \quad (5)$$

Podobný jednoduchý vztah aditivity platí ještě pro třetí centrální momenty μ_3 , zatímco pro čtvrté momenty platí [2]

$$\mu_{4,h} = \mu_{4,f} + 6 \mu_{2,f} \mu_{2,g} + \mu_{4,g} \quad (6)$$

V analýze difrakčních profilů se velmi často užívá druhý centrální moment – variance, nejen díky rovnici (5), ale taky díky své přímé fyzikální interpretaci [3]. Na užitečnost čtvrtých momentů v profilové analýze bylo upozorněno v [4]. Více pozornosti věnovali čtvrtým momentům autoři [5], zejména k určování velikosti částic, mikrodeformací a obsahu uhlíku v martenzitu z jedné difrakční linie. Jejich postup byl použitý k určení velikosti částic a mikrodeformací z jedné linie při studiu plastické deformace kovů [6]. V příspěvku bude pozornost zaměřena zejména na tuto problematiku.

1. H. Cramér, *Mathematical Methods of Statistics*. Princeton: Princeton University Press. 1946.
2. A. Fingerland, *Czech J. Phys.*, **B 10**, (1960), 233.
3. A.J.C. Wilson, *Proc. Phys. Soc.*, **80**, (1962), 286, **81**, (1963), 41, **82**, (1963), 986.
4. G.B. Mitra, *Brit. J. Appl. Phys.*, **15**, (1964), 917.
5. A.S. Kagan & V.M. Snovidov, *Fizika metallov i metallovedeniye*, **19**, (1965), 191.
6. J. Neumann & M. Čermák, *Čs. čas. fyz.*, **A 27**, (1977), 601.

Tato práce vznikla v rámci realizace projektu Grantové agentury České republiky, číslo 106/07/0805.

PANALYTICAL USER'S MEETING

EXPERIENCE FROM ALMELO LABORATORY

Z. Matěj^{1*}, J. F. Woitok², A. Kharchenko², R. Kužel¹, V. Holý¹¹Department of Condensed Matter Physics, Faculty of Mathematics and Physics, Charles University in Prague, Ke Karlovu 5, 121 16 Praha 2, Czech Republic²PANanalytical, Lelyweg 1, P.O. Box 13, 7600 AA Almelo, The Netherlandse-mail*: matej@karlov.mff.cuni.cz**Samples**

Various types of x-ray optics in different diffraction geometries were tested on three types of samples: a high quality epitaxial layer of GaMnAs, polycrystalline Cu samples prepared by severe plastic deformation and magnetron sputtered TiO₂ nanocrystalline thin films. The aim of the project was to test selected x-ray optics modules and try to measure in nonconventional experimental arrangements as well as study structure of the samples.

Position sensitive detectors X'Cellerator and PIXcel

Both position sensitive detectors (PSDs) X'Cellerator and a prototype of new detector PIXcel were available on an horizontal MRD system. The MRD system with the selected incidenc beam optics (a hybrid monochromator or a stand-alone mirror) was used mainly for high resolution experiments and parallel beam applications. Hence we utilized these detectors for reciprocal map measurements (Fig. 1 and 2) and for a measurement in the parallel beam geometry with a low take-off angle (Fig. 5).

Comparison of Hybrid and 1 monochromators

The 2X Hybrid Mirror/Monochromator was used for the high resolution measurements of the GaMnAs layer sample. The intensity gain was excellent with good angular resolution (Fig. 3). Only for higher diffraction angles ((006) diffraction) the broad spectral band-pass of the monochromator induced a significant broadening of the GaAs substrate peak.

Both monochromators, the Hybrid and the Alpha1, were tested on polycrystalline Cu samples prepared by severe plastic deformation. The intensity of the focusing Alpha1 monochromator was very good, it was possible to utilize all advantages of the focusing symmetrical geometry (prog. slits, PSD detector). The shape of the peaks profiles was really nice (Fig. 4, potentially of enough quality to make possible evaluation of the dislocation density and arrangement). The intensity from the Cu sample measured by the 2X Hybrid Monochromator was lower. It is, however, necessary to consider that for this bulk polycrystalline sample the used parallel beam setup is not a good option. Just a very small part of the sample is irradiated in the symmetrical scan. It is not possible to use any PSD detector. On the other hand in comparison with the Bartels Monochromators available in the MFF x-ray laboratory the intensity gain from the Hybrid Monochromator is much higher,

hence also powder samples can be measured with excellent resolution.

Applications of the Alpha1 and the Hybrid Monochromators is well described in the X'Pert PRO User's Guide.

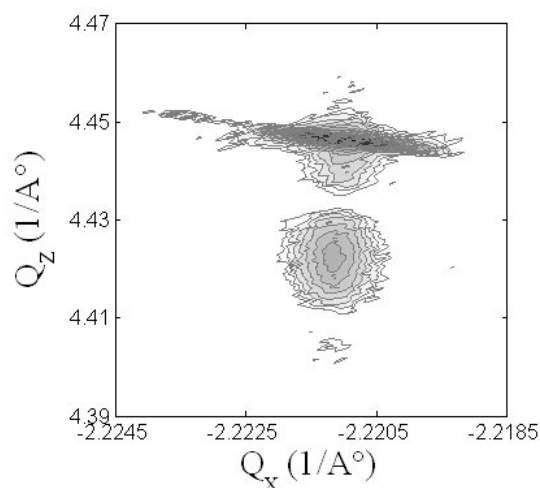


Figure 1. GaMnAs (204), Hybrid Monochromator, Triple axis analyzer, 15 h, note that the (204) is a weak diffraction for Zinc Blende type semiconductor structures

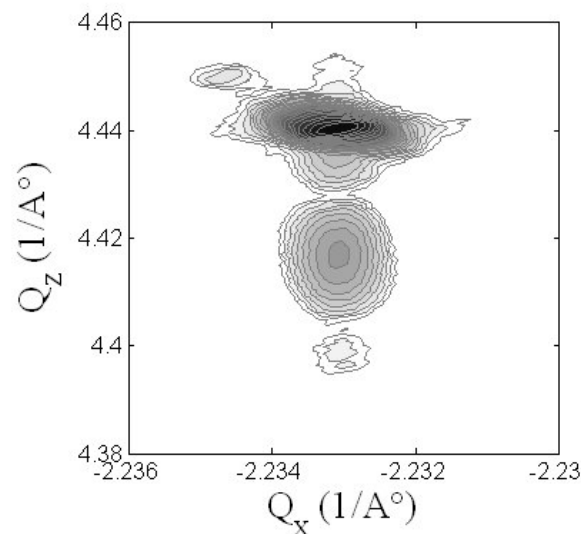


Figure 2. GaMnAs (204), Hybrid Monochromator, PIXcel, 2 h 20 min, 4x higher absolute intensity than with TA (Fig. 1)

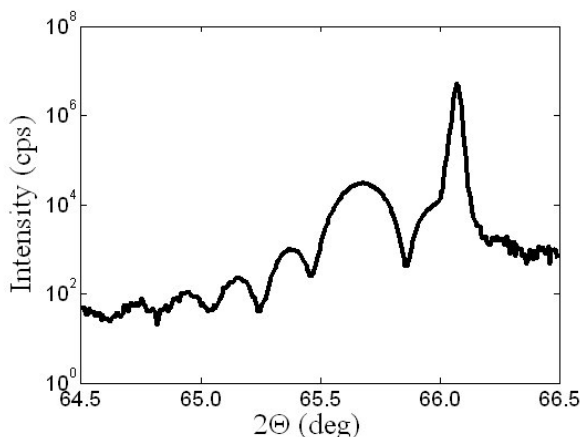


Figure 3. (004) diffraction of GaMnAs (50 nm), MPD, 2X Hybrid Monochromator, Mirror in the Diff. beam, 10 min.

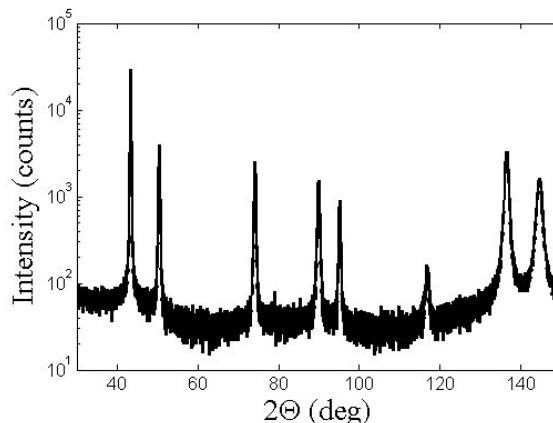


Figure 4. ECAP(1x) Cu sample, Alpha1 system, X'Celerator, 13 h.

Measurement of thin films - grazing incidence vs. grazing exicidence

The aim of this experiment was mainly to check usefulness of a PSD detector in the parallel beam geometry for study of polycrystalline thin films. To achieve a good resolution instead of the 2Theta scan with a low incidence angle the experiment was done in the grazing exit geometry. The scan, a little bit unconventional in the Data Collector software, with a same step in the both angles, incident angle Omega as well as the diffracted angle 2Theta, was performed. The PSD detector was measuring spectra for some range of diffraction angles 2Theta for each step of the scan.

Hence a series of 2Theta scans for different take-off angles $\text{Alpha}_f = 2\text{Theta} - \text{Omega}$ were acquired (Fig. 6). The exit angles were really low – close to zero. It should be possible to evaluate layer structure of the sample, however, it is complicated by texture.

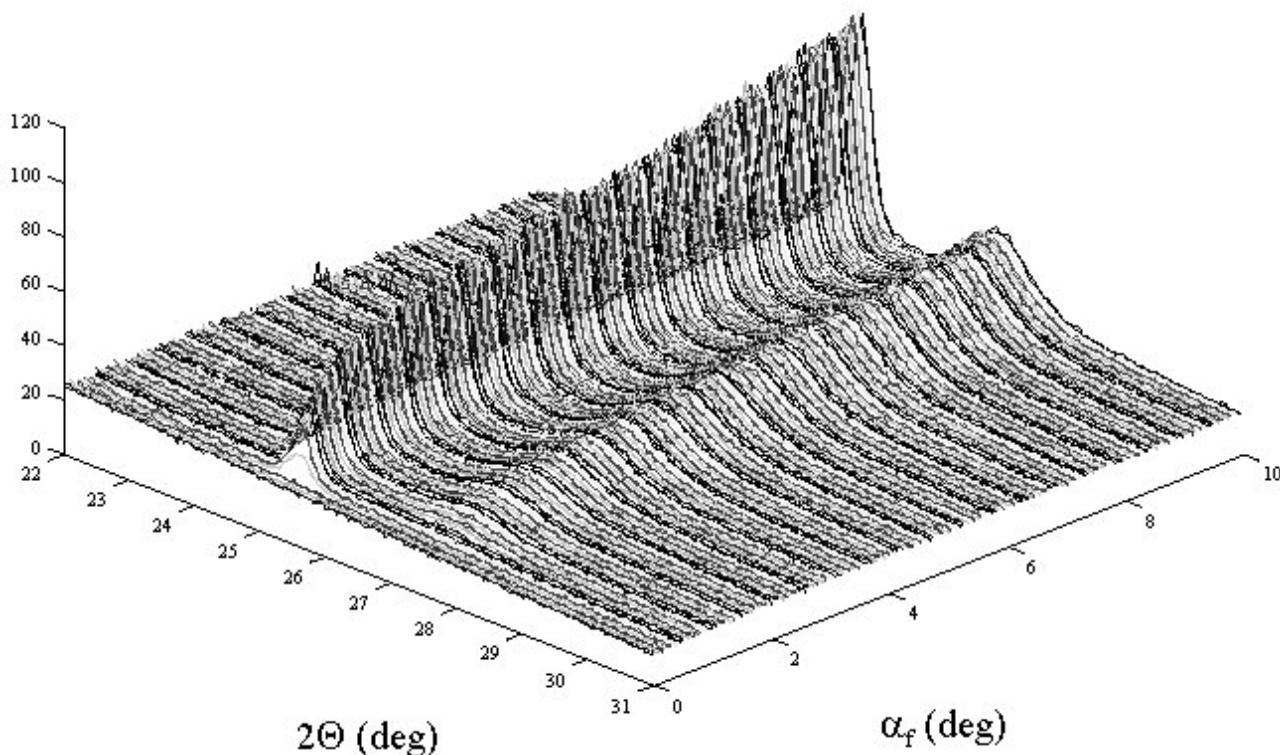


Figure 5. TiO2 thin film on Si substrate: Part of the measured spectra with the PSD in the low exit angle geometry. Anatase (101) – the higher peak at the lower 2Theta angle, Rutile (110) – the lower peak at the higher 2Theta angle; range of the exit angle: 0 – 10 deg.

MICRO-DIFFRACTION WITH A MONO-CAPILLARY: HOW TO SETUP OUR EXPERIMENT

P. Bezdička, E. Kotulanová

*Institute of Inorganic Chemistry AS CR, v.v.i., 250 68 Husinec-Řež, Czech Republic
petrb@iic.cas.cz*

The experimental setup of a micro-diffraction experiment has already been described elsewhere [1]. One of the most important aspects of the micro-diffraction experiment is the alignment of a sample.

The spot on the sample that is to be analyzed can be determined by means of an alignment microscope. This microscope is attached to a PreFIX interface and it is equipped with a cross-hair in the ocular. This setup permits one to adjust samples with a precision of about 50 μm . There is no way how to store the “*in situ*” information about the analyzed point or even about the precision of the system alignment.

Therefore we decided to modify this experimental setup using the alignment microscope. Together with IntracoMicro, Ltd. we constructed an optical interface for accommodation of a video camera in the position of the microscope eyepiece (fig. 1).



Figure 1. Mintron MTV-62W1P camera equipped with an optical interface.

This interface is equipped with a similar cross-hair that is also aligned with the optical system of our X'PertPRO diffractometer. Therefore it could be used in the same way as an optical eyepiece. Either an analog or a digital video camera with a $\frac{1}{3}$ " sensor and C/CS lens can be used with this interface. The choice of a camera depends on what is the main purpose of the use of such attachment. If it is the preference of a good documentation of experiments, a digital camera may be in preference, as it permits the production of photographs with a better resolution and better reproduction of colors. If it is necessary to check the alignment of the system that needs to visualize the trace of the primary beam on the surface of a fluorescence disk, the analog camera, with its superior sensitivity, is absolutely necessary. The use of such a camera (with the sensitivity better than 0.01 Lux) can be very useful for a routine check of the system. An inferior resolution and color inaccuracy are the drawbacks of that choice.

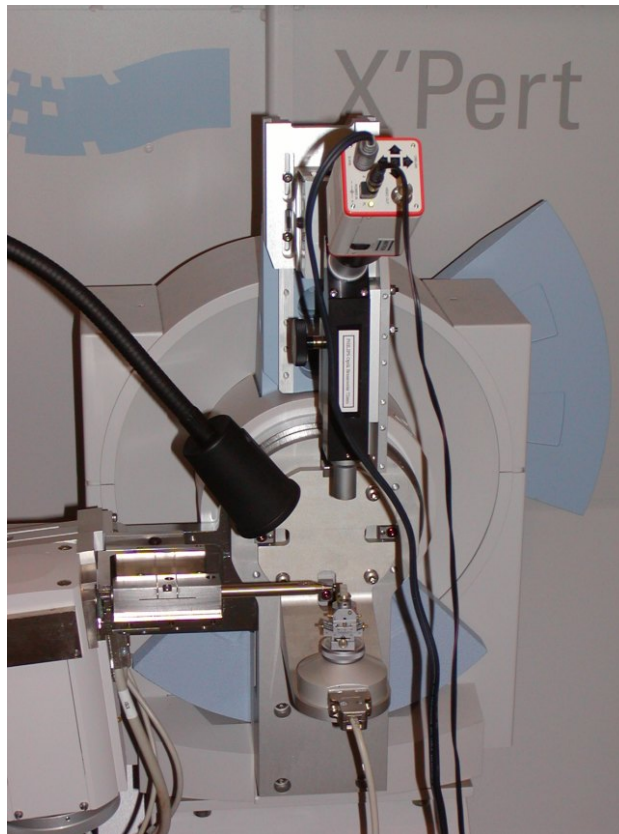


Figure 2. A video camera installed in the X'PertPRO diffractometer

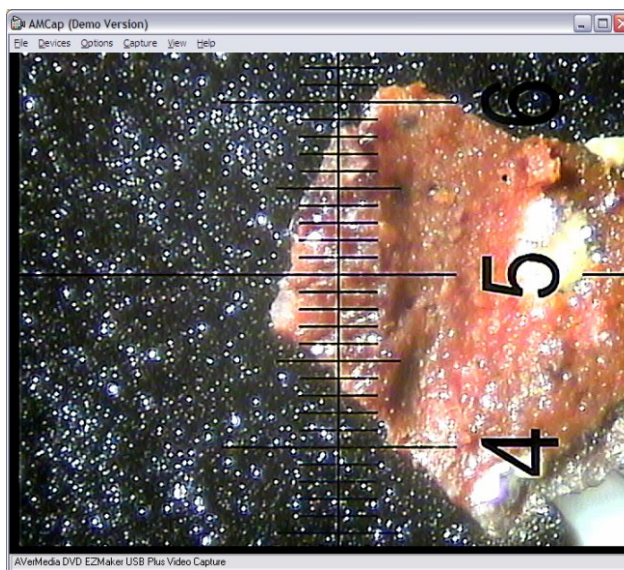


Figure 3. A typical photograph of the aligned sample that is to be analyzed.



After consideration of all benefits and drawbacks of the use of either an analog or a digital camera, we decided to install for our system the analog "Mintron MTV-62W1P" camera (fig. 1) with the minimum sensitivity of 0.007 Lux.

The overview of the experimental setup installed on our X'PertPRO diffractometer is shown in the figure 2.

Figure 3 shows a typical sample of a fragment that has been placed on a Si zero background sample holder and set up for X-ray powder micro-diffraction with the analyzed point (cross-hair)

The X-ray micro-diffraction with a conventional X-ray tube, focusing mono-capillary with a diameter of 0.1 mm,

and a position-sensitive detector allows analysis of fragments as well as polished cross sections that permits us to deal with samples routinely prepared for optical or electron microscopy. The use of a video system for alignment of such samples significantly enhances the accuracy of positioning of samples and permits a routine check of adjustment of the whole system.

1. V. Šimová, P. Bezdička, J. Hradilová, D. Hradil, T. Grygar, *Powder Diffract.*, **20**, (2005), 224.

TEXTURE AND STRESS MEASUREMENT WITH THE EULERIAN CRADLE ON MRD SYSTEM, DOUBLE-MIRROR SETUP

R. Kužel

Department of Condensed Matter Physics, Faculty of Mathematics and Physics, Charles University in Prague, Ke Karlovu 5, 121 16 Praha 2, Czech Republic

Measurement with Eulerian cradle

For complete texture and stress analysis, it is necessary to measure reflections not only from the lattice planes parallel to the surface as in Bragg-Brentano symmetrical θ - 2θ scans or at specific inclinations like e.g. for parallel beam 2θ scans. Instead, information from large scale of inclinations is necessary. Either their diffraction peak intensities (for texture) or positions (for stress) are required. Traditionally Eulerian cradles are used for this purpose in combination with point focus of the tube and collimators. However, big disadvantage of this arrangement is significant defocussation and also loss of intensity. Therefore in modern diffractometers polycapillaries are used behind the X-ray tube which produce transforms divergent beams into a beam parallel in all directions. There is still some divergence there but the suppression of defocusing effects and gain in intensity is significant. The arrangement can be in principle seen on Fig. 1 which differs only in one element, the Goebel mirror should be replaced by polycapillary module

for texture and stress measurement (of course, also the tube should be rotated by 90° in order to use point focus).

Not only full texture measurement but also fast θ or ω scans can easily be done with the cradle.

Two software packages are available from Panalytical – X'Pert Texture and X'Pert Stress.

Texture software provide basic functions for display of pole figures in several views (Figure 2) and calculation of ODF – Orientation Distribution Function. Unfortunately, there not many options for example for precise scaling of the plots and their export. Nevertheless, basic needs of texture characterization are met.

On the other hand, stress software is very user-friendly. It allows both automatic and manual data processing and very fast and flexible stress evaluation not only in approximation of uniaxial stress (nonlinearity in \sin^2 plot, triaxial stress). Database of elastic constants for some materials can be used and modified by the user.

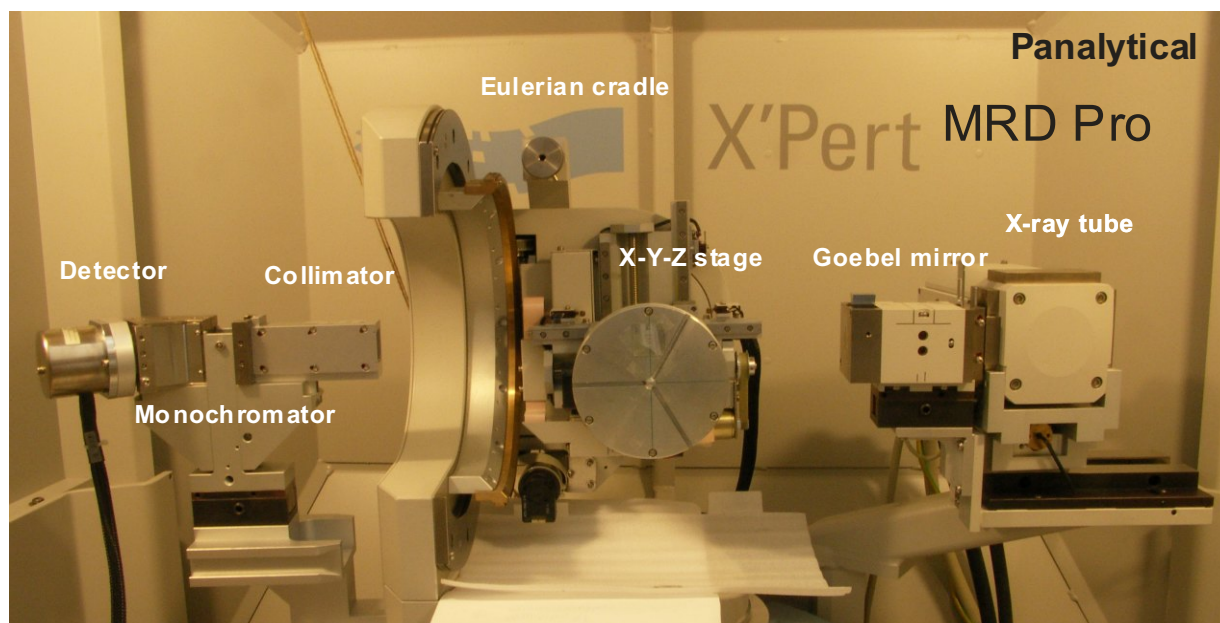


Figure 1. Photo of MRD Pro system with Eulerian cradle.

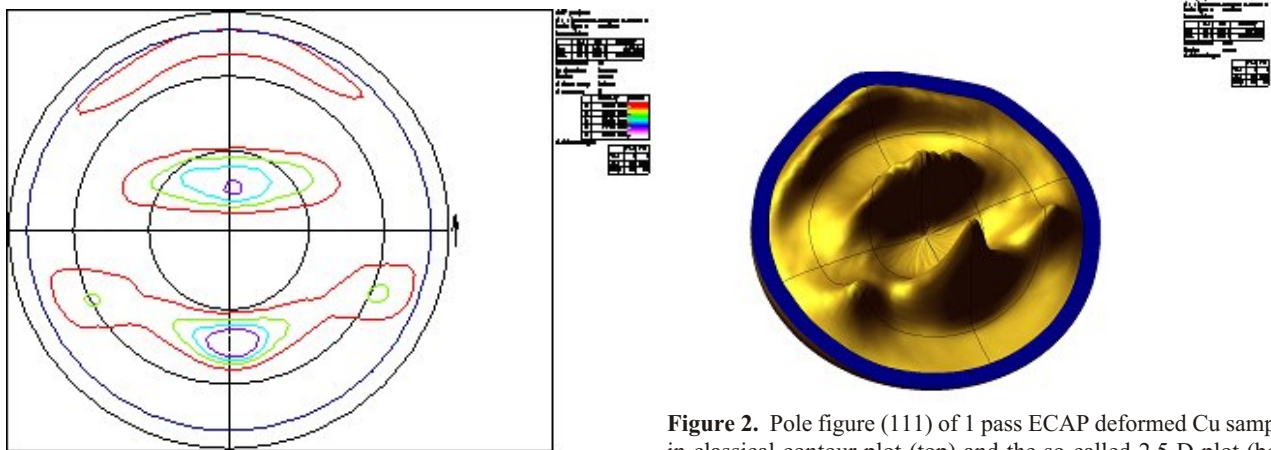


Figure 2. Pole figure (111) of 1 pass ECAP deformed Cu sample in classical contour plot (top) and the so-called 2.5 D plot (bottom).

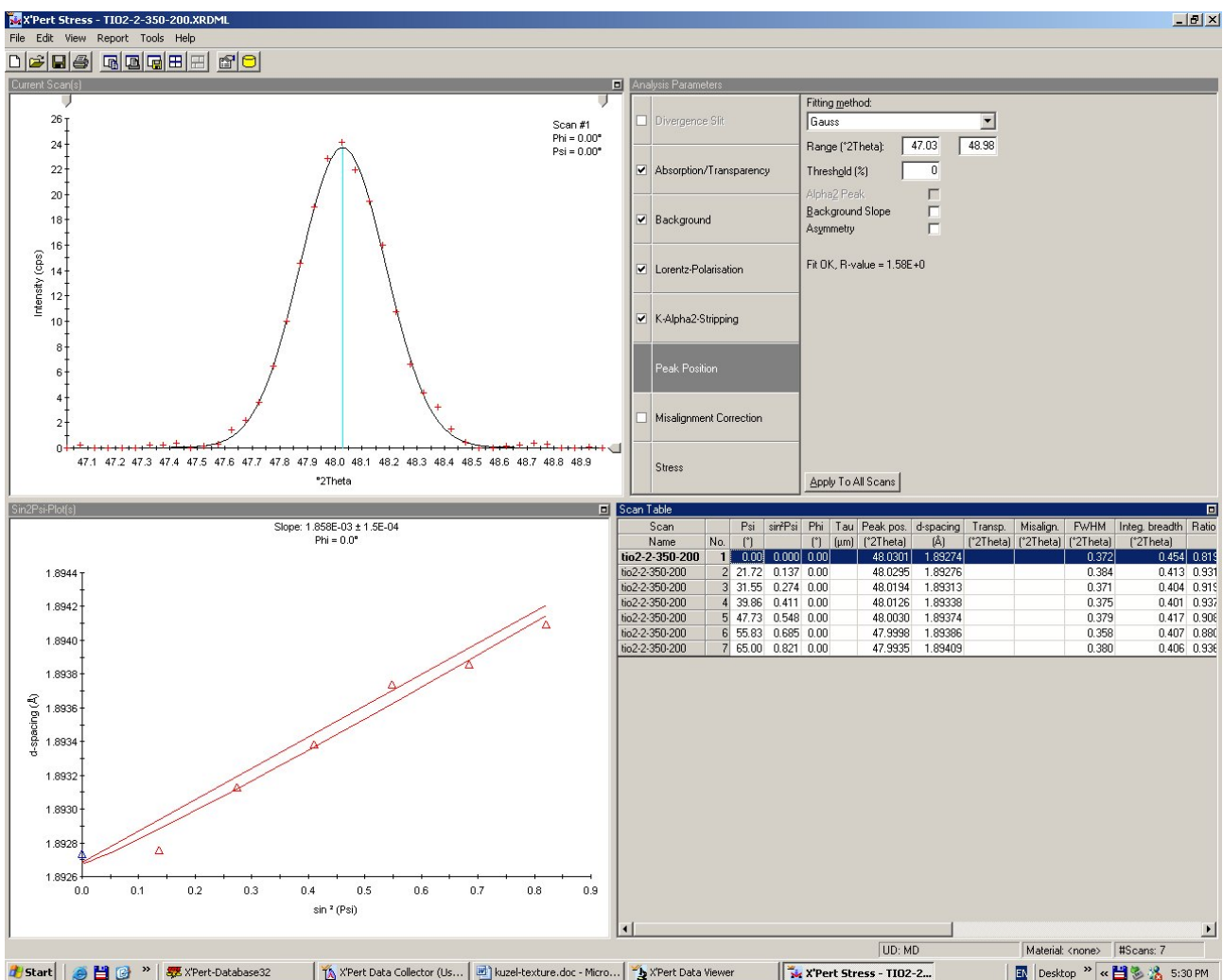


Figure 3. Basic screen of X'Pert Stress. Peak positions are determined automatically for all measured lines but the position of each individual peak of $\sin^2\psi$ plot (left bottom) can be determined by different algorithm (center of gravity, parabola, Gauss, Lorentz, Pearson, pseudo-Voigt function, manually). The following corrections can be applied – absorption, transparency, Lorentz-polarization, misalignment, K_2 stripping.

Double-mirror setup

Nowadays, the measurement using parallel beam and Goebel mirror is more or less routine especially for thin films, when 2 scans with small angles of incidence are required. This arrangement gives quite high intensity but

rather poor resolution that is 3-4 times worse than for conventional Bragg-Brentano focusing geometry. In case of nanocrystalline films this is not that big problem because physical broadening is significantly higher. However, for films with better crystallinity and not so high strains, the



physical broadening is close to the instrumental one. In this case, the insertion of the second mirror in the diffracted beam can help. It converts the parallel beam to convergent one and resulting resolution is back close to the one of B-B setup. Picture of the setup on X'Pert Pro vertical system is on Fig. 4.

When to use this setup? In all cases, when high resolution and parallel beam on the sample are required simultaneously

Thin film studies with low angles of incidence. In this case, there is one significant disadvantage – the acceptance of the second mirror is very limited (to about 1.5 mm) so that the useful sample area is limited by this dimension. It lead to intensity drop and may cause difficulties for samples with large grains

When precise specimen positioning in the goniometer axis is difficult – irregularly shaped surface, rough surface, usage of different chambers. In such cases, even symmetrical - 2 scans may be of interest. They give not much lower intensities than focusing BB setup with similar resolution. It is well known that focusing geom-

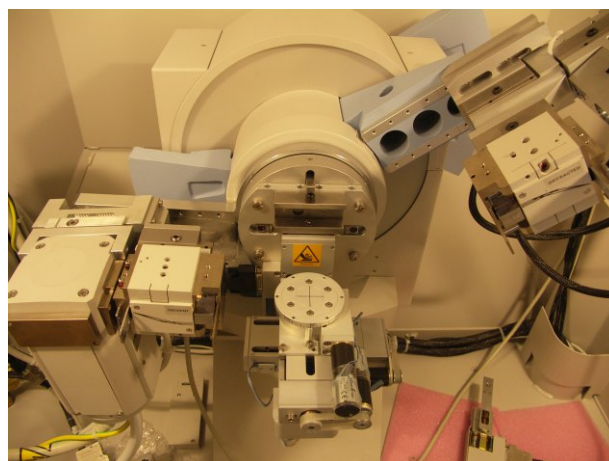


Figure 4. Double-mirror setup on vertical diffractometer.

etries are very sensitive to careful alignment. Double-mirror setup can overcome this drawback.

KURS PROTEINOVÉ KRYSTALOGRAFIE

CRYSTALLIZATION METHODS USED IN PROTEIN CRYSTALLOGENESIS

Ivana Kutá Smatanová^{1,2}

¹*Institute of Physical Biology University of South Bohemia Ceske Budejovice, Zamek 136, 373 33 Nove Hrad, Czech Republic*

²*Institute of Systems Biology and Ecology Academy of Science of the Czech Republic, Zamek 136, 373 33 Nove Hrad, Czech Republic
e-mail: ivas@greentech.cz*

Finding suitable crystallization conditions is the main problem to solve a protein structure by X-ray diffraction techniques.

In this lecture:

classical crystallization techniques based on evaporation used for screening and optimization of crystallization conditions utilizing the screening upon previously successful chemical cocktails,

advanced counter-diffusion technique that allows the screening for crystallization conditions in a wide range of supersaturation while suppressing concentration, of protein and precipitant,

cross-crystallization procedure based on using additives to modify crystal morphology and to improve diffraction quality,

will be discussed.

Literature:

Ivana Tomčová and Ivana Kutá Smatanová: Copper co-crystallization and divalent metal salts cross-influence effect – a new optimisation tool improving crystal morphology and diffraction quality. *Journal of Crystal Growth*, accepted for publication (2007).

Ivana Tomčová and Ivana Kutá Smatanová: Cross-crystallization as a new optimization tool of crystallization procedures. *Materials Structure* 14, 1, 3-5 (2007).

Ivana Kutá Smatanová, José A. Gavira, Pavlína Řezáčová, František Vácha, and Juan M. García-Ruiz: New techniques for membrane protein crystallization tested on photosystem II core complex of *Pisum sativum*. *Photosynthesis Research* 90 (3), 255-259 (2006).

Ivana Tomčová, Rui Miguel Mamede Branca, Gabriella Bodó, Csaba Bagyinka, and Ivana Kutá Smatanová: Cross-crystallization and preliminary diffraction analysis of a novel di-heme cytochrome *c₄*. *Acta Cryst.* F62, 820-824 (2006).

Julie Wolfova, Rita Grandori, Erika Kozma, Neal Chatterjee, Jannette Carey and Ivana Kuta Smatanova: Crystallization of the flavoprotein WrbA optimized by using additives and gels. *Journal of Crystal Growth* 284, 3-4, 502-505 (2005).

This work is supported by the Ministry of Education of the Czech Republic (MSM6007665808 and LC06010) and by the Academy of Sciences of the Czech Republic (AVOZ60870520).



DEPOSITION OF MACROMOLECULAR STRUCTURES TO THE PROTEIN DATA BANK (PDB)

Bohdan Schneider

Center for Biomolecules and Complex Molecular Systems, Institute of Organic Chemistry and Biochemistry, AS CR, Fleming Sq. 2, CZ-16610 Prague, Czech Republic

Most grant agencies and virtually all journals require that the result of crystallographic or solution NMR analysis are deposited with a public database. In case of macromolecular structures, it is the Protein Data Bank ([1], PDB, <http://www.pdb.org/>) or the Nucleic acid Database ([2], NDB, <http://ndbserver.rutgers.edu>). Everyone involved in structure determination should keep in mind that structures that have been nurtured in laboratories for months and in some cases for years, will not be viewed in light of notebooks, log files from data processing and refinement, neither from endless coffee discussions in the laboratory but solely by their representation in the PDB. The deposition process therefore deserves attention and should be viewed as an important part of structure determination. The workshop will present the tools developed by the RCSB PDB that assist and simplify the deposition.

The main deposition tool is AdIt, deposition and validation tool, <http://deposit.rcsb.org/>. It is a web-based mmCIF editor. To deposit a structure, the user uploads the relevant coordinate and experimental data files and then adds any additional information. Each structure should be validated before deposition. Coordinates should be checked for format consistency and for quality of valence geometry using the Validation server (<http://deposit.pdb.org/validate/>). Web server <http://pdb-extract.rcsb.org/auto-check/> allows non-trivial checking of coordinates versus x-ray diffraction data („structure factors“) using programs SFCheck, REFMAC, and CNS. Correctly formatted coordinates as well as collection and refinement statistics should be produced by the `pdb_extract` tool ([1], <http://pdb-extract.rcsb.org/>) that allows integration of refinement logs of most major refinement programs into PDB and/or mmCIF format and significantly thus simplifies the deposition. Identity of ligands present in the to-be-deposited structure should be verified using the ligand tool, currently at the web for „Ligand Depot“ (<http://ligand-depot.rcsb.org/>) that allows you to determine whether your ligands are cor-

rectly labeled, whether the right atom names were used, and whether these ligands are possibly new to the PDB.

All the mentioned web pages have available extensive tutorials, many steps have context-sensitive help and example pages and most of them are available as downloadable executable files as well as source codes.

The workshop will show deposition process using example files, possibly from participants.

Acknowledgement

The PDB project is funded by the National Science Foundation, the Department of Energy, the National Institute of General Medical Sciences, and the National Library of Medicine. BS kindly acknowledges support by a grant from the Ministry of Education of the Czech Republic No. LC512 for the Center for Biomolecules and Complex Molecular Systems.

1. Berman H.M., Battistuz T., Bhat T.N., Bluhm W.F., Bourne P.E., Burkhardt K., Feng Z., Gilliland G.L., Iype L., Jain S., Fagan P., Marvin J., Padilla D., Ravichandran V., Schneider B., Thanki N., Weissig H., Westbrook J.D., Zardecki, C. (2002): The Protein Data Bank. *Acta Crystallogr D*, **58**, 899-907.
2. Berman H.M., Olson W.K., Beveridge D.L., Westbrook J., Gelbin A., Demeny T., Hsieh S.-H., Srinivasan A.R., Schneider B. (1992): The Nucleic Acid Database—a comprehensive relational database of three-dimensional structures of nucleic acids. *Biophys. J.* **63**, 751–759.
3. Yang, H., Guranovic, V., Dutta, S., Feng, Z., Berman, H.M., Westbrook, J.D. (2004): Automated and accurate deposition of structures solved by X-ray diffraction to the Protein Data Bank. *Acta Cryst. D* **60**, 1833-1839.
4. Feng, Z., Chen, L., Maddula, H., Akcan, O., Oughtred, R., Berman, H.M., Westbrook, J. (2004): Ligand Depot: a data warehouse for ligands bound to macromolecules. *Bioinformatics* **20**, 2153-2155.







SOME COMMERCIAL PROGRAMS FOR STRUCTURE VISUALIZATION

R. Kužel

Charles University in Prague, Faculty of Mathematics nad Physics
Ke Karlovu 5, 121 16 Praha 2

Keywords:

molecular structure visualization, crystal structure visualization

Abstract

There are several programs or software packages available for structure visualization. A survey of some of them has been published in Materials Structure [1]. In this contribution, some commercial systems are mentioned. They usually include interactive graphics when the structures can be easily rotated and moved by mouse. There are many visualization options of structures, calculation of bond lengths and angles and as a rule also calculations and visualization of powder diffraction pattern. Four systems are characterized in the review - Crystal Impact software, Crystal Maker, Crystal Studio and Crystallographica including licensing options.

Crystal Impact software

Software company Crystal Impact [2] distributes molecular and crystal structure visualization software **Diamond**. In addition to structural pictures it also offers an extensive set of functions that let easily model any arbitrary portion of a crystal structure from a basic set of structural parameters (cell, space group, atomic positions). It supports both crystal and molecular structures (i.e. with and without translational symmetry). Each structure set can contain: atomic parameters, cell parameters and space-group (optional), anisotropic displacement parameters, chemical and bibliographic data (author, reference, database origin, etc.). Supports multiple structure pictures for a structure data set. It allows importing of number of different formats (e.g. CIF, SHELX, XYZ, CRYSTIN etc.). Structure pictures can be exported to 3D VRML and many graphical formats of 2D pictures. Basic screen can be seen on Fig. 1.

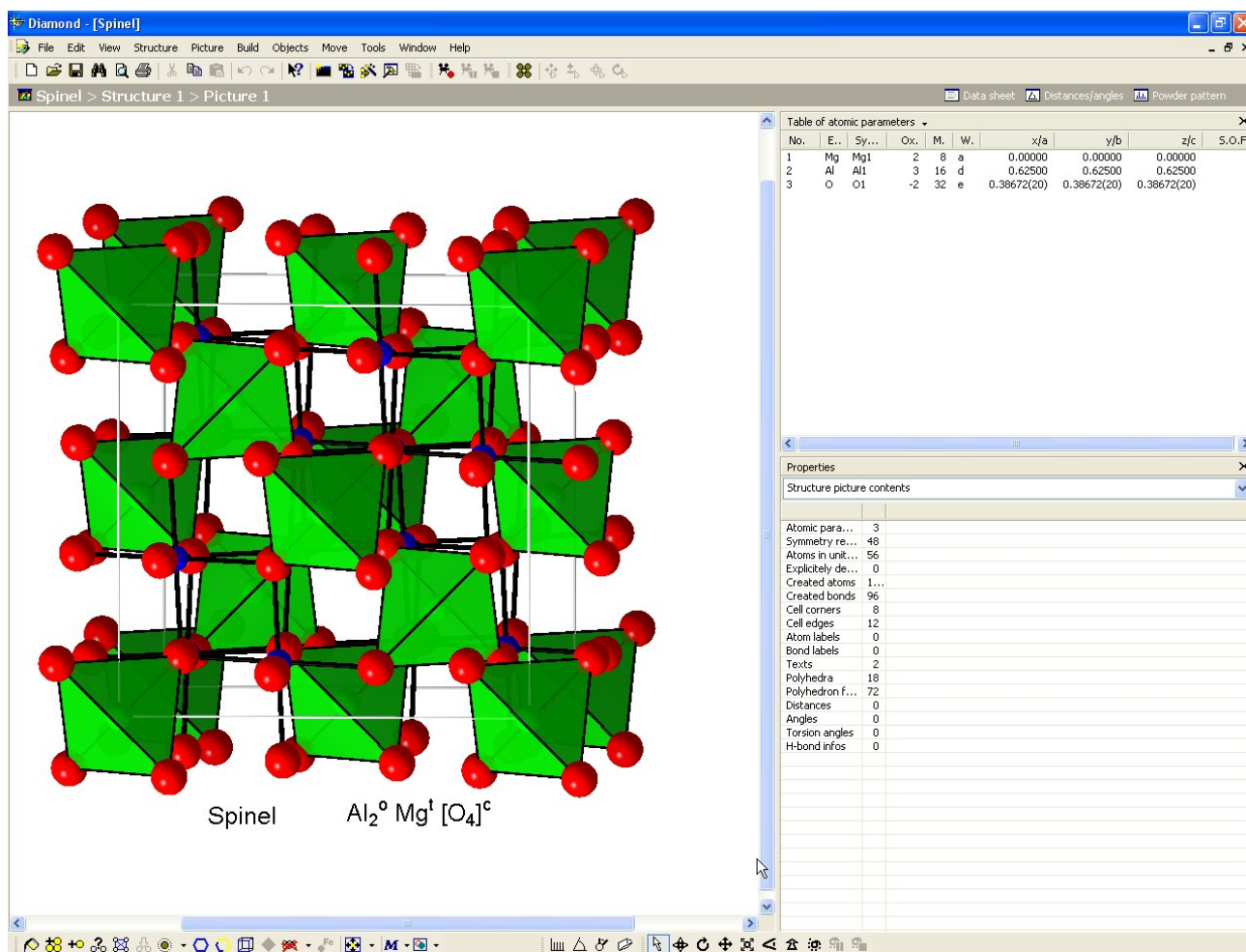


Figure 1. Basic screen of Diamond software



Diamond - [Spinel]

File Edit View Structure Picture Build Objects Move Tools Window Help

Spinel > Structure 1 > Data sheet

General

Origin ICSD
Code 31375
Database dates
Common name
Systematic name Magnesium dialuminium oxide
Structural formula Mg Al₂ O₄
Analytical formula

Bibliographic data

Author(s) Yamanaka, T, Takeuchi, Y
Publication title Order-disorder transition in Mg Al₂ O₄ spinel at high temperatures up to 1700 degrees C
Citation ZEKRDZ,165,65-78 (1983)
Mineral name Spinel
Compound source synthetic
Structure type
Creation method generated by SIMILAR 3.0
Comments

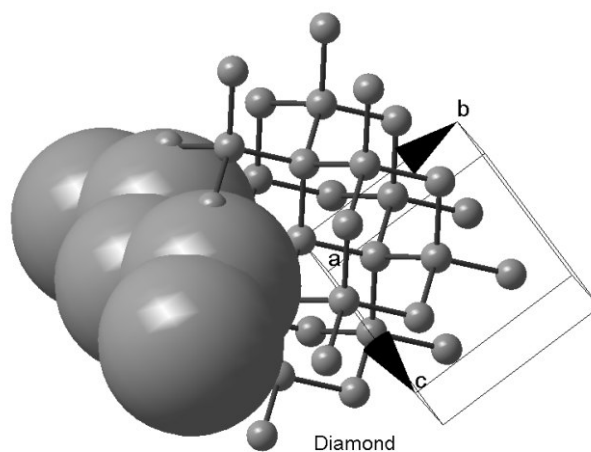
Phase data

Formula sum Al₂ Mg O₄
Formula weight
Crystal system cubic
Space-group F d -3 m (227)
Cell parameters a=8.0625(7) Å
Cell ratio a/b=1.0000 b/c=1.0000 c/a=1.0000
Cell volume 524.09(8) Å³
Z 8
Calc. density
Meas. density
Melting point
RAll 0.0248
RObs
Pearson code cF56
Formula type AB₂X₄
Wyckoff sequence eda

Atomic parameters

Atom	Dx.	Wyck.	Site	S.O.F.	x/a	y/b	z/c	U [Å ²]
Mg1	2	8a	-43m	0	0	0	0	
Al1	3	16d	-.3m	5/8	5/8	5/8		
O1	-2	32e	.3m	0.38672(20)	0.38672(20)	0.38672(20)		

Anisotropic displacement parameters, in Å²



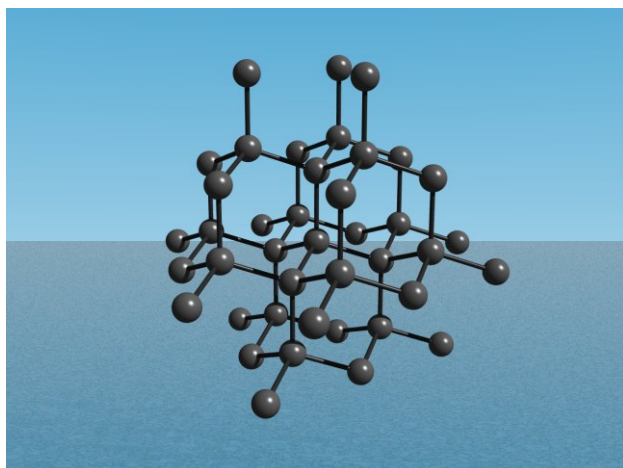


Figure 4. Rendering with external ray tracing program POVRay.

atoms, built up from selected ligand atoms, optionally with transparent or hatched surfaces.

- Definition of (transparent) lattice planes and (best) planes or lines through selected atoms.
- Adding of vectors to atoms to indicate e.g. a magnetic moment.
- Generation of H-bonds.
- Alternative color differentiation to visualize oxidation numbers, site occupation factors etc.

Animation:

- Movement of structure picture: Modes: rotation along x -, y -, and/or z -axis, horizontal and/or vertical shift within drawing area, variation of enlargement factor (from Angstroms to centimeters),
- variation of camera distance (perspective impression). Controlled by: Mouse (the faster the mouse the faster the rotation etc.), keyboard (e.g. one degree rotation per keystroke), numerically (input through dialog).
- Optional “Spin” function, i.e. acceleration of movement.
- Continuous movement, which can be interrupted and continued.
- Walk-through mode, enabling the camera/viewer to navigate through the structure picture.
- Recorder that helps to create video sequences, e.g. as AVI files.

Exploration:

- Calculation of powder pattern: Variation of diffraction parameters: Radiation type: X-ray (laboratory, synchrotron), neutron, electron, wavelength, LP correction, 2θ range, optional profile functions - pseudo-Voigt, width. Table of reflection parameters with zoom in/zoom out and tracking through 2θ range, see Fig. 5.
- Calculation of distances and angles (incl. standard uncertainties): in a configurable table, for selected atom types and a sizeable distances range, around the atom(s) currently selected in structure picture, graphical repre-

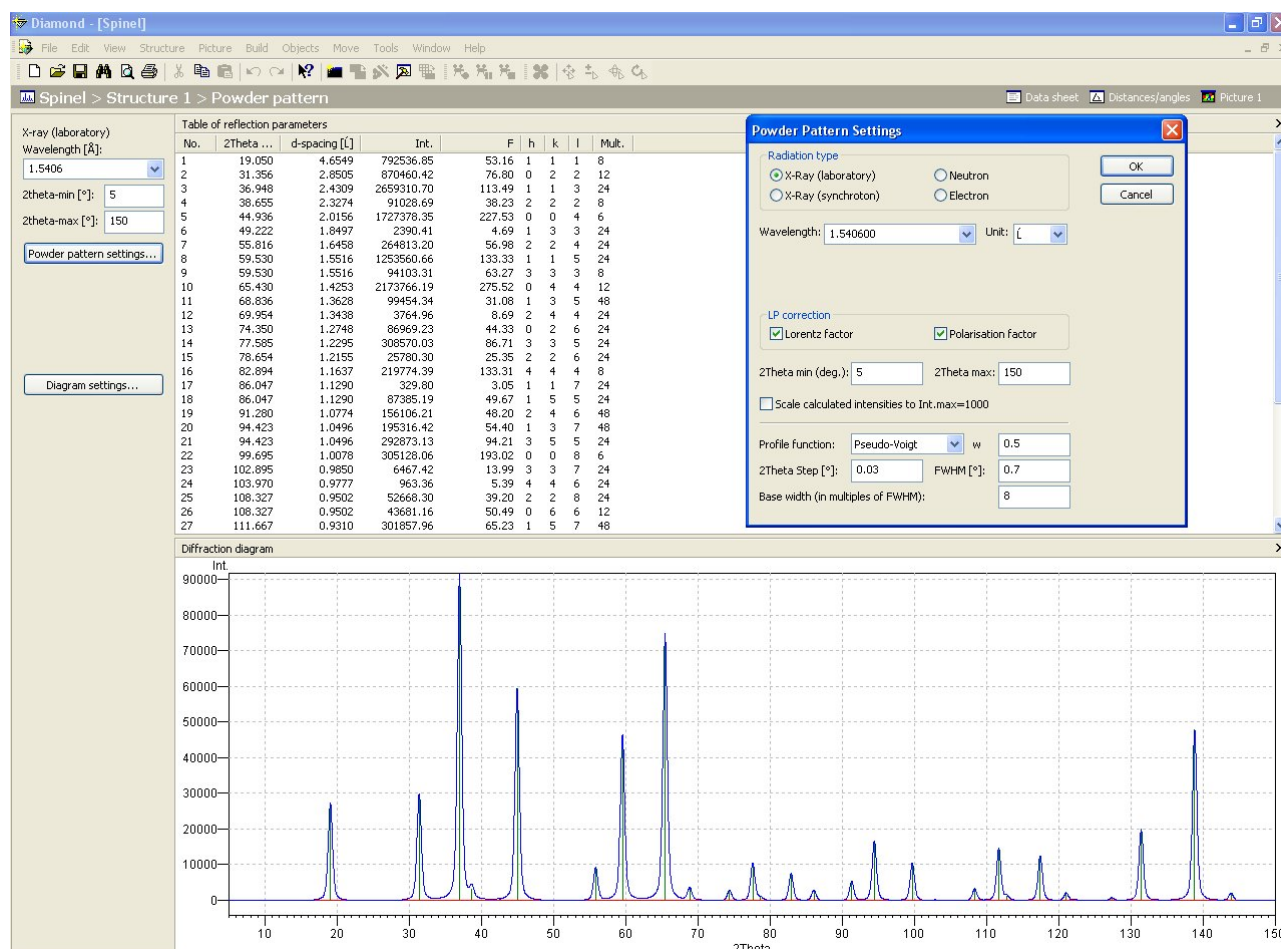


Figure 5. Diffraction pattern window of Diamond

sensation of distances as histogram with color-coded distances.

- Measuring of distances, angles, and torsion angles interactively (incl. standard uncertainties).
- Measuring of extended geometric features (incl. standard uncertainties): Angle between two planes (by hkl or (best) plane through 3 or more atoms), angle between two lines, angle between a normal of a plane and a line, distances of atoms from a plane or a line, centroid of a set of atoms, planarity or linearity of a set of atoms (distances of constituent atoms from plane/line).
- New Properties panel, displays information about: Contents of the structure picture (how many created atoms, bonds, polyhedra, etc.), the current “formula sum”, that means the number of created atoms associated to atom groups, table of the currently selected objects, distances around the selected atom(s), distances between the selected atoms, the center of the selected atoms (centroid), planarity or linearity of the selected atoms and the deviations of the atoms from that plane or line, table of atoms assigned to the selected atom of parameter list or selected atom group, table of bonds assigned to the selected bond group (i.e. atom group pair), ligand, edges, and faces informations of the selected polyhedra.

Price of single academic licence is 500 Euro, site licence (one institute or department) 1000 Euro, campus licence 2000 Euro.

Other useful software offered by Crystal Impact is *Endeavour* designed for the solution of crystal structures from powder diffraction data. The concept implies a com-

bined global optimization of the difference between the calculated and measured diffraction pattern and of the potential energy of the system.

Match! is an easy-to-use software for phase identification from powder diffraction data. It compares the powder diffraction pattern of your sample to a database containing reference patterns in order to identify the phases which are present. Both ICDD products can be used for database source.

Pearson's Crystal Data is a new crystallographic database (see also [3]).

All the above Crystal Impact software can be found on demo CD distributed for all the conference participants.

Crystal Maker Software

Crystal Maker software is distributed in two versions for Mac an PC, respectively [3].

CrystalMaker visualizing software for molecular and crystal structures is by features similar to Diamond. The interactive graphics is significantly faster on slower computers. It has the ability to display massive structures (up to 2 billion atoms). Bonds and polyhedra are automatically calculated, with the option of bond distance output and error propagation, as well as direct visualization of cluster shells and coordination networks.

In general, the program may have not all the possibilities of Diamond but it seems to be very user-friendly and nice to work with. Everything is smooth. Main window is shown on Fig. 6. One can easily switched on/off individual types of atoms from the picture and history of different views is quickly accessible.

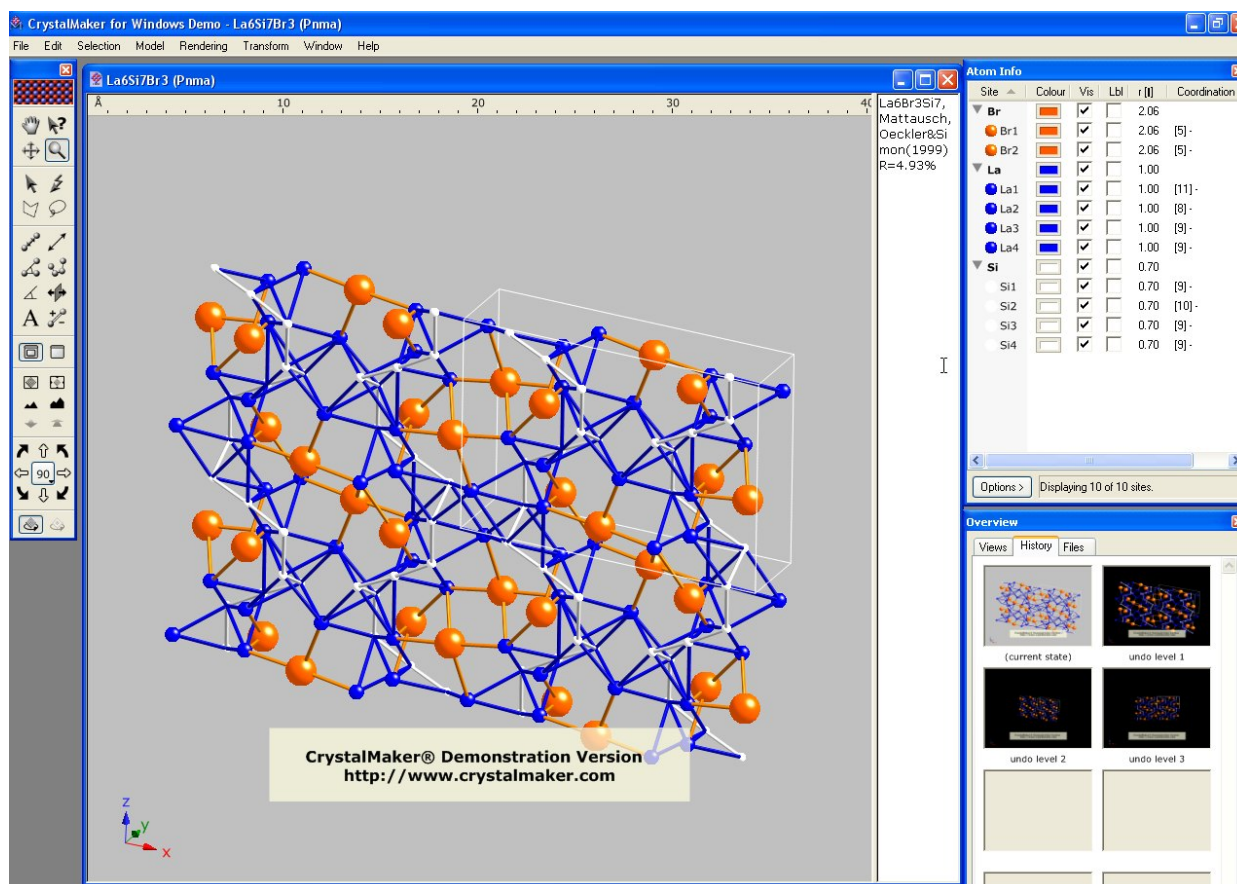


Figure 6. Main window of Crystal Maker

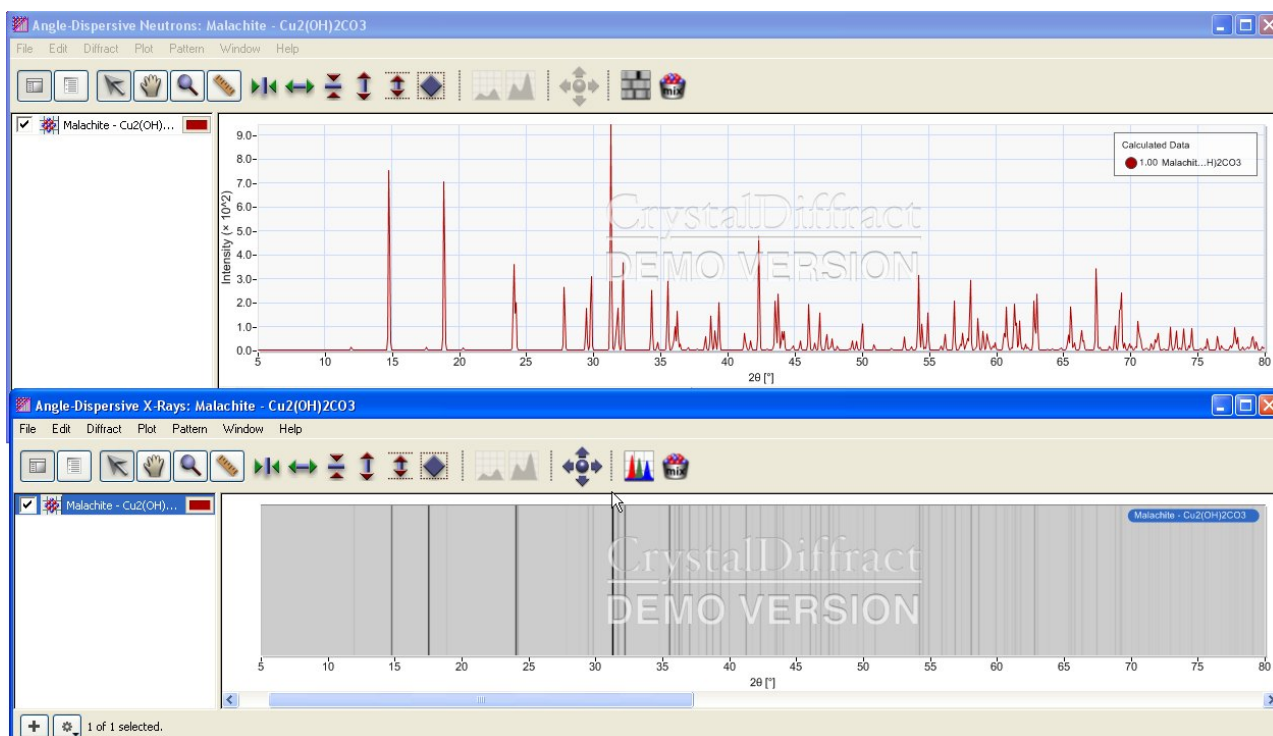


Figure 7. Two windows of CrystalDiffract - simulation of powder diffraction pattern obtained by the detector (top) and film record (bottom).

CrystalMaker is shipped with over 600 structures files, including the major rock-forming minerals plus important technological phases such as zeolites, superconductors and organic molecules. Each file is fully-annotated, with views and model types carefully chosen to highlight the salient structural features, and ready for immediate display. Animations can be saved as Quick Time movies. CrystalMaker provides photo-realistic graphics, including 3D stereo graphics (red/blue stereo glasses included with the program package).

Diffraction patterns are generated by stand-alone program *CrystalDiffract* that can be used unlike Diamond as a separate tool for simulation of powder patterns. CrystalDiffract lets simulate also patterns for multi-phase mixture; switch between X-ray or neutron radiation including time-of-flight or energy scale; visualize intensities as “films” or graphs (Fig. 7); choose different diffraction techniques; interactively edit structural and experimental parameters, and export detailed diffraction information. For shape function pseudo-Voigt function is used. Constant value of instrumental broadening can be given and in simple way also size and strain broadening.

CrystalDiffract lets edit aspects of a selected pattern’s underlying crystal’s structure, so one can determine how this affects diffraction. You can edit lattice parameters and site occupancies and also omit sites from the diffraction calculation. The Edit Crystal sheet can be resized horizontally and vertically, in order to show a range of sites and their atomic displacement parameter data (U_{ij} and U_{iso}).

In Graph mode one can use the Stack command to stack multiple diffraction patterns without danger of overlap. For a complex diffraction pattern there may be many overlapping peaks. The Overlay Peak Positions submenu allows you to identify the positions of individual diffraction

peaks. One can superimpose a series of peak markers showing the peak centres, and their relative intensities.

Of course, very important feature is a possibility to load experimental data (in xy format) and compare them with the simulation. CrystalDiffract work well together with CrystalMaker.

The third part of the software package is *SingleCrystal*. It lets simulate electron diffraction patterns, display sections of the reciprocal lattice and work with stereographic projections. One can manipulate diffraction patterns in real time, changing the orientation of a crystal, the scale or intensity saturation. It is possible to measure intensities, distances and angles on screen. There is even a unique option of visualizing the phases of diffracted beams, via colour-coded diffraction spots.

Educational pricing of the software is the following: single licence - CrystalMaker 350 Euro, CrystalDiffract 150 Euro, SingleCrystal 99 Euro.

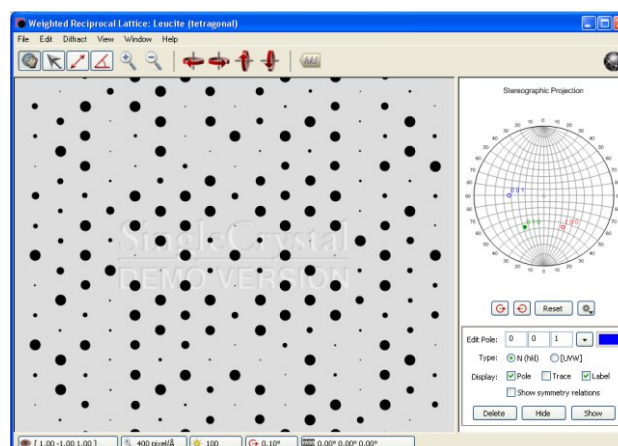


Figure 8. Screen of the program SingleCrystal.

Crystallographica

The package is distributed by Oxford Cryosystems [4, 5] and it includes structure and reciprocal lattice display, powder simulation, graphing (including common x-ray data formats) and a unique crystallographic scripting language, all supported numerous example scripts and structures as well as free unlimited technical support.

Crystallographica is essentially a visualisation program, consisting of a series of tools for setting and displaying a multitude of properties of a crystal structure. Some of these tools are highly visual in nature: the program incorporates a structure drawing package, reciprocal lattice display and powder pattern simulation. A set of dialogs allow not only crystal properties to be set, but also provide quick and easy methods for viewing crystal properties.

All these features are shared by the Lite and Full versions of Crystallographica. The Full version adds a unique crystallographic scripting language based on pascal syntax which allows a whole new level of flexibility and power to the program. This language is fully integrated with the other tools, and may be used for anything from calculating simple properties to creating animations. Four typical windows are shown on Fig. 9.

Integrated crystal structure drawing package allows a number of views of the same structure or else comparison

of different structures. Plots can be examined using the mouse and keyboard to rotate and zoom the image, or controlled precisely from the Interpreter.

VRML files can be exported, showing crystal structure and including anisotropic displacement ellipsoids, polyhedra and crystal planes.

Integrated viewer allows the reciprocal lattice to be displayed in a variety of styles. Viewing direction may be synchronised with other such windows and with structure display.

Flexible X-ray and neutron powder diffraction pattern simulation including Rietveld-style control over peak shape and width area available. Simulated pattern may be compared with experimental data in the graphing tool. Profile and peak data may be exported to file. Scripting language includes utilities for combining plots to form multi-phase patterns or residuals.

A set of simple and easy-to-use dialogs provides a powerful user interface to access atom properties, contents of asymmetric unit, cell parameters, bond lists, crystal symmetry (via space group or list of generators), radiation, reflection lists, powder simulation and VRML options.

Pascal interpreter supports variables, arrays, records, sets, functions and procedures. Extensions to core Pascal include exponential operator, dynamic sizing of arrays and enhanced string handling. The interpreter may be

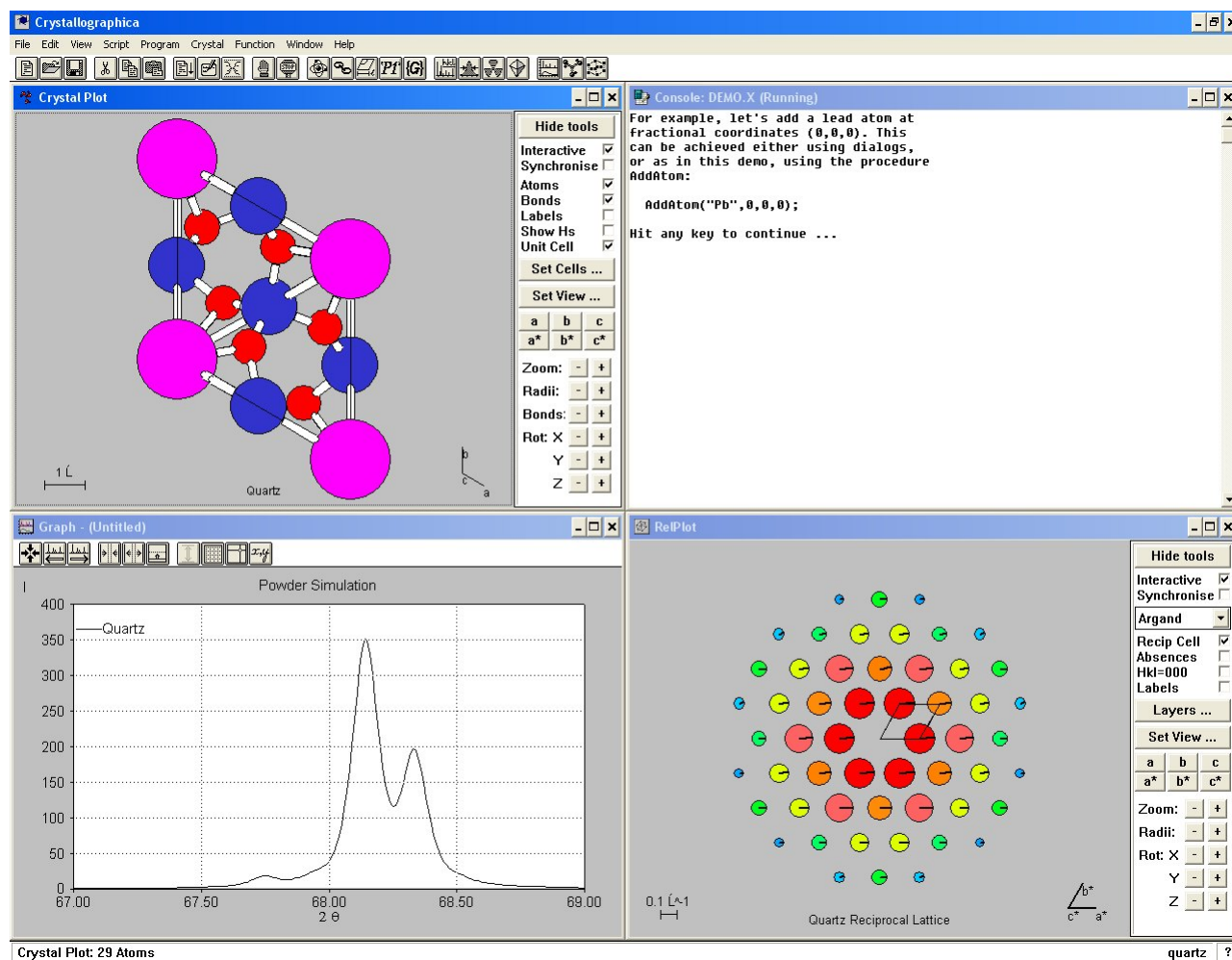


Figure 9. Crystallographica windows showing interactive structure picture (top left), command line window of the scripting language (right top), part of diffraction pattern (left bottom) and reciprocal lattice (right bottom).

used interactively or called to run scripts contained in text files.

A library of several hundred crystallographic routines covering atom properties, bonding, cell parameters, symmetry, radiation, reflections, powder simulation, crystal structure drawing and graph plotting.

User-scripted routines are easily integrated, so that the system can be customised.

A set of databases holding information on X-ray and neutron scattering factors including dispersion corrections, absorption factors, X-ray wavelengths, bonding radii, elemental properties and space group symmetry.

Academic single user pack costs 500 GBP (lite version without interpreter - 250 GBP), teaching pack - site licence is for 1000 GBP.

Crystal Studio

This is a software by Australian CrystalSoft corporation [6]. Apart from providing normal crystallography functionalities like 3D graphics etc. as other packages, Crystal Studio offers ample functions for *defects like dislocations, twin boundaries and stacking faults, interfaces and surfaces and two phase coherent combinations*. It also covers XRD, neutron and electron diffraction simulations and reciprocal lattice. Moreover it especially simulates the combined zone axis diffraction patterns for twins and two phase coherent combinations.

As in the preceding programs different visualization options are available: ball and stick model, stick model, space filling model, ellipsoid and stick model, ball and stick plus translucent space filling model, mixed model, *ribbon model*, perspective or orthographic projection. Vectors can be added to the atoms.

Crystal Studio is integrated with a crystallographic database. The database contains information about all 530 space group specifications from various versions of International Tables for (X-Ray) Crystallography, information on all elements in the Periodic Table including valence, radii etc. and latest data for atomic scattering amplitude and Debye-Waller factors for diffraction calculations. The database also include a crystal structure database and a layer/cluster database. Non-standard space group specifications can be created and added to the database by user. The 530 existing space group specifications can also be modified by users. Crystal structures without space group specifications can also be created, built and stored in the database.

The program is distributed in several versions - Lite, Standard, Professional, Enterprise with academic pricing starting from 450 to 1300 US\$ for single licence and 1900 US\$ for 5 user site licence.

Acknowledgement

This contribution was partially supported within the framework of the program MSM 0021620834 financed by the Ministry of Education of the Czech Republic.

References

1. M. Hušák, *Materials Structure*, **10**, 1a (2003) 17.

2. <http://www.crystalimpact.com/>
3. R. Kužel, S. Daniš, *Materials Structure*, v. **14** (2007).
3. <http://www.crystallmaker.co.uk>
4. <http://www.oxfordcryosystems.co.uk/>
5. <http://www.crystallographica.com/>
6. <http://www.crystalsoftcorp.com>

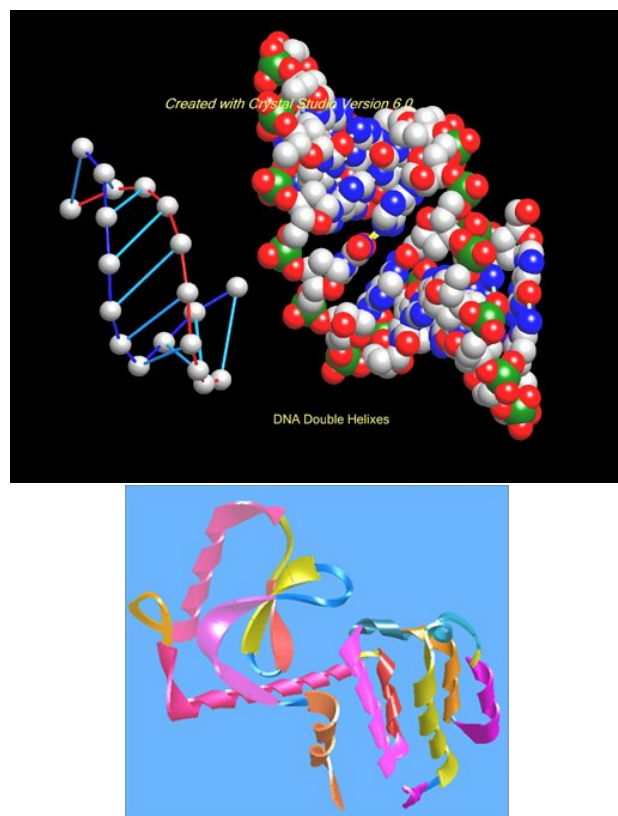


Figure 10. Different models for visualization in CrystalStudio.

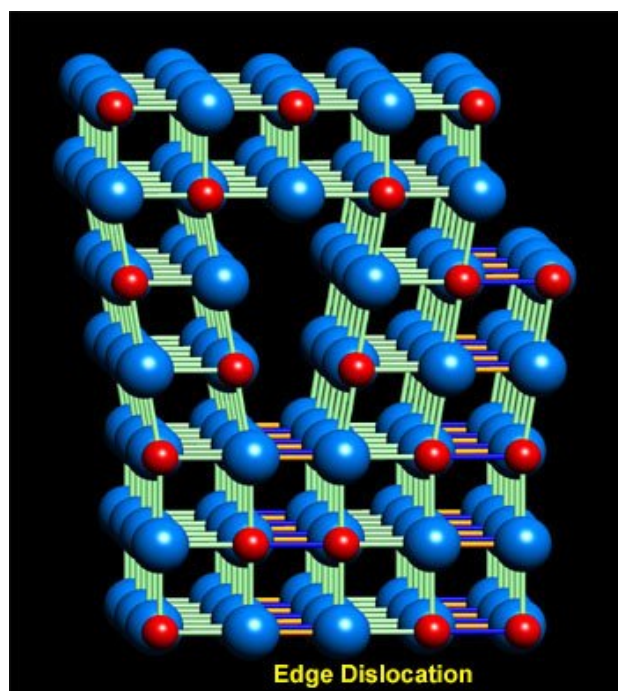


Figure 11. Visualization of dislocation in the lattice by CrystalStudio.

